Genomic basis of drought resistance in *Fagus sylvatica*

Markus Pfenninger[1,2,3], Friederike Reuss[1], Angelika Kiebler[1], Philipp Schönnenbeck[4], Cosima Caliendo[1,4], Susanne Gerber[4], Berardino Cocchiararo[3,5], Sabrina Reuter[6], Nico Blüthgen[6], Karsten Mody[6,11], Bagdevi Mishra[7], Miklós Bálint[3,8,9], Marco Thines[3,7,10], Barbara Feldmeyer[1]

[1] Molecular Ecology, Senckenberg Biodiversity and Climate Research Centre, Frankfurt am Main, Germany

[2] Institute for Organismic and Molecular Evolution, Johannes Gutenberg University, Mainz, Germany

[3] LOEWE Centre for Translational Biodiversity Genomics, Frankfurt am Main, Germany

[4] Institute for Human Genetics, University Medical Center, Johannes Gutenberg University, Mainz, Germany

[5] Conservation Genetics Section, Senckenberg Research Institute and Natural History Museum Frankfurt, Gelnhausen, Germany

[6] Ecological Networks lab, Department of Biology, Technische Universität Darmstadt, Darmstadt, Germany

[7] Biological Archives, Senckenberg Biodiversity and Climate Research Centre, Frankfurt am Main, Germany

[8] Functional Environmental Genomics, Senckenberg Biodiversity and Climate Research Centre, Frankfurt am Main, Germany

[9] Agricultural Sciences, Nutritional Sciences, and Environmental Management, Universität Giessen, Giessen, Germany

[10] Institute for Ecology, Evolution and Diversity, Johann Wolfgang Goethe-University, Frankfurt am Main, Germany

[11] Department of Applied Ecology, Hochschule Geisenheim University, Geisenheim, Germany

Abstract

In the course of global climate change, central Europe is experiencing more frequent and prolonged periods of drought. These drought events have severe and detrimental impacts on the forest ecosystem. The drought years 2018 and 2019 affected European beeches (*Fagus sylvatica* L.) in noticeably different ways: even in the same local stand, badly drought damaged trees immediately neighboured apparently healthy trees. This led to the hypothesis that the genotype rather than the environment was responsible for this conspicuous pattern. We used this natural experiment to study the genomic basis of drought resistance in a Pool-GWAS approach. Contrasting the extreme phenotypes, we identified 106 significantly associated SNPs throughout the genome. The majority of affected genes was previously implicated in drought reaction in other plant species. Most observed

non-synonymous changes led either to a substantial functional amino acid exchange or a stop-codon. A SNP-assay with 70 informative loci allowed the successful prediction of drought phenotype from the multilocus genotype in 98.6% in a validation sample of 92 trees with Linear Discriminant Analysis. Drought resistance in European beech appeared to be a moderately polygenic trait that should nevertheless respond well to natural selection, selective management, and breeding. The widespread distribution of drought resistance across natural beech populations represents an important argument for maintaining genetic diversity in dynamic forest ecosystems. The results from this study could therefore contribute to harness beech wood forests against ongoing climate change.

Keywords

Genome-wide association study, genomic prediction, forest tree, Fagales, conservation genomics, functional environmental genomics

Introduction

Climate change comes in many different facets, amongst which are prolonged drought periods (Christensen et al. 2007). The Central European droughts in the years 2018 and 2019 caused severe water stress in many forest tree species, leading to the die-off of many trees (Schuldt et al. 2020). Among the suffering tree species was European beech, *Fagus sylvatica* L. As one of the most common deciduous tree species in Central Europe, *F. sylvatica* is of great ecological importance: beech forests are a habitat for more than 6,000 different animal and plant species (Brunet et al. 2010) ; Dorow *et al.* 2010). The forestry use of beech in 2017 generated a turnover of more than 1 billion € in Germany alone (Thünen Institute 2020), without taking the economic and societal value of the ecosystem services of woods into account (Elsasser *et al.* 2016). However, the drought years 2018 and 2019 severely impacted the beech in Germany (Paar & Dammann 2019). Official reports on drought damages in beech recorded 62% of trees with rolled leaves and 20-30% of small leaves, mainly in the crown, resulting in 7% of badly damaged or dead trees. As shown before (Bressem 2008), most trees affected from drought stress were medium to old aged.

Under favourable conditions, beech is a competitive and shade tolerant tree species, dominating in mixed stands (Pretzsch *et al.* 2013). High genetic diversity within populations supports adaptation to local conditions (Kreyling et al. 2011). Significant differences between local populations in tolerance to various stress factors such as early frost (Czajkowski & Bolte 2006), drought (Cocozza *et al.* 2016; Harter *et al.* 2015) or air pollution (Müller-Starck 1985) are known. The distribution of *F. sylvatica* is limited by water-availability, as the tree does not tolerate particularly wet or dry conditions (Sutmöller *et al.* 2008). It is therefore quite conceivable that the species could suffer even more under the predicted future climatic conditions than today.

Despite the widespread, severe drought damages, a pattern observed in all beech forests was very noticeable (personal observations). Not all trees in a beech stand were equally damaged or healthy, but the damage occurred in a mosaic-like pattern instead. Even though the extent of drought damage varied among sites, apparently completely healthy trees immediately neighboured severely damaged ones and *vice versa*. This observation gave rise to the hypothesis that it were not the local environmental conditions that might be decisive for the observed drought damage, but rather the genetic make-up of the individual trees.

We decided to draw on this natural “experimental set-up” to infer the genomic basis underlying the drought susceptibility in *F. sylvatica*. We identified more than 200 neighbouring pairs of trees with extreme phenotypes and used a Pool-GWAS approach (Bastide *et al.* 2013) to infer associated SNP loci by contrasting allele frequencies with replicated pools of drought susceptible and resistant individuals. In addition, we individually re-sequenced 51 pairs of susceptible and resistant trees. If

the observed pattern indeed has a genetic basis, identification of the associated loci would enable the genomic prediction of drought resistance (Stocks *et al.* 2019). Constructing a SNP assay from the most highly phenotype associated SNPs, we validated 70 identified loci by predicting the drought phenotype of an additional set of beech trees from their genotype at these loci using Linear Discriminant Analysis. With this accurate genomic prediction tool, e.g., the choice of drought resistant seed producing trees and selective logging could help accelerate and monitor natural selection and thus harness beech forests against climate change (Waldvogel *et al.* 2020).

Results

Sampling, climate development and phenotyping

Damaged and healthy beech tree pairs were sampled from lowland Rhein-Main plain, the adjacent low mountain ranges of Odenwald and Taunus, and mountain ranges from Central and Northern Hessen (Fig. 1A). When summarising the climatic conditions from 1950 to 2019 for the sampling sites in a principal component analysis (PCA), the sites were divided into two groups by axis 1, a temperature gradient. The sites in the Taunus mountains grouped with those from the northern part of Hessen, while the Rhein-Main plain clustered with the sites from the Odenwald (Fig. 1B). This grouping was also used to construct the GWAS pools (see below). Comparing the climate from the 1950s, when most of the trees sampled were already in place, with the decade from 2010-2019, showed that all local conditions changed substantially and similarly in the direction and extent of warmer and drier conditions (Fig. 1B). The steepest temperature increase occurred in the 1980s, while precipitation patterns changed mostly in the last decade (Suppl. Fig. 1). A wide range of parameters, potentially relevant as selection pressures changed drastically during this period: the mean January daily minimum temperature at the sampling sites increased by 1.49°C from -2.64°C (s.d. 1.68°C) in the 1950s to -1.15°C (s.d. 2.50°C) during the last decade. The mean August daily maximum temperatures increased even more by 2.37°C from 22.06°C (s.d. 1.95°C) to 24.43°C (s.d. 2.35°C). Simultaneously, mean annual precipitation decreased by 40.5 mm or 5.5% from 741.2 mm (s.d. 85.8 mm) to 700.7 mm (s.d. 70.9 mm). Most of the precipitation loss (84%) occurred during the main growth period between April and September, with a decrease of 33.9 mm from 410.4 mm (s.d. 36.1 mm) to 376.5 mm (s.d. 25.6 mm).

Mean monthly evaporation potential, available from 1991 onwards, showed that, compared to the beginning of the 1990s, the main growth period of beech from April to September became increasingly drier, with up to 30 mm more evaporation per month. The drought dynamics suggested that the years 2018 and 2019 were not outliers, but rather part of a long-term, accelerating trend (Fig. 1C), following the overall global pattern (Trenberth *et al.* 2014) .

Phenotypic measurements generally confirmed the study design and selection of trees: healthy and damaged trees within each tree pair did not differ significantly in *trunk circumference*, *tree height*, *canopy closure* and *competition index* (Fig. 2 A-D), hence these parameters were not considered in further analyses. As expected, and confirming the assignment of damage status, the quantity of *dried leaves* and *leaf loss* differed substantially between damaged and healthy ones (Fig. 2 E-F, Suppl. Table 2).

Linkage disequilibrium, population structure and genome-wide association study

For 300 beech trees we generated four DNA pools from two climatically distinct regions (North and South Hessen, Fig. 1B), contrasting trees that were either healthy or highly drought damaged respectively (Tab. S1). The “South” pools consisted of 100 individuals each, whereas the “North” pools contained 50 individuals each. We created ~50GB 150 bp-paired end reads with insert size 250-300 bp on an Illumina HiSeq 4000 system per pool. More than 96% of the reads mapped against the

128 repeat-masked chromosome level beech reference genome (accession no.). After filtering the
129 alignment for quality and a coverage between 15x and 70x, and removing indels, allele frequencies
130 for 9.6 million SNPs were scored. All 100 individuals from the North population were additionally
131 individually re-sequenced to ~20x coverage each (for more details see M&M). This data was used to
132 a) determine individual variability in allele frequencies and b) to validate the information content of
133 the candidate SNP-set.

134 Using the healthy South pool, we inferred the extent of genome wide linkage disequilibrium (LD;
135 (Feder *et al.* 2012)). The plot of LD r^2 against the distance from the focal SNP showed that LD fell to
136 the genome-wide background level within less than 120 bp (Fig. 3A). The PCA on SNP variation of the
137 individually re-sequenced trees from the North population explained 12.3% of accumulated variation
138 on the first two axes (Fig. 3B). Trees from the same sampling site (within the North population) did
139 not tend to cluster together (Fig. 3B). Trees within one phenotypic class were genomically not more
140 similar than between classes (Suppl. Fig. 2, ANOSIM R = -0.008, p = 0.76, 9,999 permutations).

141 Pool-GWAS analysis identified 106 SNPs significantly associated with the drought damage status
142 using a Cochran-Mantel-Haenszel test on the two pairs of damaged and healthy pools after false
143 discovery rate correction and a cut-off at 1×10^{-2} (Fig. 4A, Suppl. Fig. 3). Some of the 106 SNPs were
144 in close physical proximity (<120bp) and thus probably linked. Taking this into account, 80
145 independent genomic regions were associated with the drought damage status. None of the
146 significantly differentiated SNP loci was mutually fixed; the observed allele frequency differences
147 between healthy and damaged trees at associated loci ranged between 0.12 and 0.51 (Fig. 4B).

148 *Affected genes and gene function*

149 Of the 106 significant SNPs, 24 were found in 18 protein coding genes (Table 1). Forty-nine genes
150 were the closest genes to the remaining 82 SNPs. For 60 of these genes, the best BLAST hit was with
151 a tree, mostly from the Fagales genera *Quercus* and *Castanea* (Table 1, Suppl. Table 3). Among the 24
152 SNPs in genes, we observed 13 non-synonymous changes. For eleven of these, the alternate allele
153 was associated with the damaged phenotype and only in two cases with the healthy. Three of the
154 non-synonymous substitutions resulted in a stop codon, and of the remaining ten, eight exchanges
155 caused a major change in amino acid characteristics and thus probably in protein folding or function
156 (Table 1). One gene, a PB1 domain-containing protein tyrosine kinase, contained four non-
157 synonymous changes, suggesting that the allele version associated with the damaged phenotype lost
158 its function (Tab. 1). From the 18 genes with significant SNPs, functional information could be
159 obtained from the UniProt database for 13 (Suppl. Table 3). Of these, nine genes were associated in
160 previous studies with either environmental stress response (two) or specifically with drought stress
161 response (seven; Suppl. Table 2). Of the 49 predicted genes closest to the remaining significant SNPs
162 (Tab. 1), 16 could be reliably annotated (Suppl. Table 2). Twelve had been directly related to drought
163 in previous studies, while three were previously associated with other environmental stress
164 responses (Suppl. Tab. 3).

165 *Genomic prediction*

166 We furthermore set out to determine how many SNPs were needed to successfully predict the
167 drought susceptibility of individual trees, i.e. to develop a genotyping assay. All Pool-GWAS SNPs in
168 addition to the top 20 individual re-sequencing SNPs were used to create a SNP combination to reach
169 a genotyping success threshold of min. 90%. Seventy loci proved to be suitable for reliable
170 genotyping with a SNP assay. On average, each of the 95 individuals was successfully genotyped at
171 67.7 loci (96.7%). We coded the genotypes as *0* for homozygous reference allele, *1* for heterozygous
172 and *2* for the homozygous alternate allele, thus assuming a linear effect relationship. Figure 5 shows

173 the genotypogram for the tested individuals. Linear discriminant analysis (LDA) correctly predicted
174 the observed phenotype from the genotype in 91 of 92 cases (98.9%). Prediction success decreased
175 to 65% when successively removing loci from the analysis (Suppl. Fig. 4). Nevertheless, ordering the
176 individuals according to the LDA score of axis 1 revealed no clear genotype pattern that distinguished
177 healthy from damaged trees (Fig. 5). Observed heterozygosity at loci used in the SNP assay of
178 individuals in the upper half of predictive values for a healthy phenotype was not significantly
179 different from heterozygosity of the lower half (Suppl. Fig. 5). Ordering the loci according to their
180 squared loadings showed that the contribution of loci to the genomic prediction differed
181 substantially (Fig. 5). As expected, the histogram of LDA scores showed two peaks, corresponding to
182 the two phenotypes (Suppl. Fig. 6).

183 Discussion

184 Over the last two decades, increasing drought periods caused severe damage to European forests
185 (Schuldt et al. 2020; Pretzsch 2012). Conifers seem to suffer the most, but also deciduous trees were
186 strongly affected (Schuldt et al. 2020). Weather data from our study area from 1950 onwards
187 suggested that the climatic conditions for beech trees changed dramatically during this period.
188 Roughly estimating the tree age from their trunk circumference (Bošeľa *et al.* 2014), more than a
189 third of the trees were already in place at the beginning of this period. About 60% were recruited
190 prior to the acceleration of temperature change from the 1980s onwards. As a result, trees in the
191 mountainous regions of the study area today experience climatic conditions comparable to those
192 experienced by low land trees in the 1950s, which in turn now experience a climate that used to be
193 typical for regions much further South. Given the documented propensity of beech for local
194 adaptation (Gárate-Escamilla *et al.* 2019; Pluess *et al.* 2016; Aranda *et al.* 2015), including drought
195 (Bolte *et al.* 2016), it is therefore conceivable that current conditions exceed the reaction norm of
196 some previously locally well-adapted genotypes with detrimental consequences for their fitness. If
197 the trend of an increasingly drier vegetation period persists, this will likely affect an even larger
198 proportion of the currently growing beeches.

199 Evolutionary genomics will be indispensable to predict and manage the impact of global change on
200 biodiversity (Waldvogel *et al.* 2020). As already shown for other partially managed (tree) species
201 (Stocks *et al.* 2019), in particular pool-GWAS approaches (Endler *et al.* 2016) have proven to be useful
202 to guide conservation management. Our strictly pairwise sampling design avoided many pitfalls of
203 GWAS studies, arising, e.g., from cryptic population structure and shared ancestry (Hoban *et al.* 2016;
204 Wellenreuther & Hansson 2016). As expected from previous studies, we found no population
205 structure among the sampling sites (Rajendra *et al.* 2014). Applying relatively strict significance
206 thresholds, we found systematic genomic differences between the healthy and damaged trees. In all
207 cases, these differences were quantitative and not categorical, i.e. we found allele frequency changes
208 but no fixed SNPs between phenotypes. Significant SNPs were mostly not clustered - we found on
209 average 1.4 selected SNPs in a particular region. These findings were in line with the observed very
210 short average LD in *F. sylvatica,* indicating that polymorphisms associated with the two phenotypes
211 were likely old standing genetic variation (Harris & Nielsen 2013). Moreover, such SNPs are therefore
212 mostly detached from the background in which they arose. They are often the actual causal variants.
213 This observation is underlined by the high proportion of non-synonymous significant SNPs within
214 genes, which in most cases caused substantial, likely functional or conformational changes in the
215 proteins. Interestingly, most of the allelic variants associated with a healthy phenotype were also the
216 variants in the reference genome. This might be due to the choice of the *F. sylvatica* individual from
217 which the reference genome was gained. This more than 300-year-old individual is standing at a
218 particularly dry site on a rocky outcrop on the rim of a scarp where precipitation swiftly runs off.
219 Trees at such sites were likely selected for drought tolerance.

None of the genes found here was involved in a transcriptomic study on drought response in beech saplings (Müller *et al.* 2017). However, most of the reliably annotated genes with or close to SNP loci significantly associated with drought phenotypes had putative homologs in other plant species previously shown to be involved in drought or other environmental stress response (for citations see Suppl. Table 2). The involvement of in total 67 genes together with the effect size distribution suggested that drought resistance in *F. sylvatica* is a moderately polygenic trait, which should respond well to artificial breeding attempts and natural selection. However, given the relatively strict threshold criteria, it is likely that more yet undetected loci contribute to the respective genotypes. The low LD in beech predicts that an adaptation to drought will not compromise genome-wide genetic diversity.

We achieved a high level of accuracy using genomic data to predict the drought phenotype from individuals not used to identify drought associated SNP loci. This suggested that we mainly identified alleles that are widespread throughout the sampled range and not locally specific. In addition, we confirmed a large level of genetic variation in the sampled regions. The observation that trees with the highest predictive values showed no loss of heterozygosity indicated that there is still adaptive potential for drought adaptation in the species. With the SNP assay, we therefore created a tool that can i) support the choice of seed trees for reforestations, ii) provide decision guidance for selective logging and iii) monitor, whether natural selection is already acting in the species.

Material and Methods

Sampling and phenotyping

In August/September 2019, we sampled leaf tissue of 402 *Fagus sylvatica* trees from 32 locations in Hessen/Germany (set 1, Figure 1). In August 2020, additional 53 trees from four sites were sampled (set 2, Figure 1). The coordinates and characteristics of each site can be found in Suppl. Table 1. The sampling was performed in a strictly pairwise design. The pairs consisted of one tree with heavy drought damage of the crown (lost or rolled up, dried leaves) and one with an unaffected crown, respectively. This categorisation into least and most damaged trees was taken in comparison to the other trees in the respective forest patch. The pairs were *a priori* chosen such that the two trees were i) mutually the closest neighbours with contrasting damage status, ii) free from obvious mechanical damage, fungal infestations or other signs of illness, similar iii) in tree height, iv) trunk circumference, v) light availability, and vi) canopy closure. In addition, each pair was situated at least 30 m from the closest forest edge. For each tree of the chosen pairs, we recorded the exact position and the estimated tree height (in 1 m steps), measured the trunk circumference at 150 cm height above the ground (in 10 cm steps), and estimated the leaf loss of the crown and the proportion of dried leaves (in 5% steps). We also recorded the estimated distance (in 1 m resolution) and the specific identity of the two closest neighbour trees for each pair member and calculated a competition index C as follows: $C = S_1/D_1 + S_2/D_2$, where S_1 and S_2 are the trunk diameter at 150 cm and D_1 and D_2 the distances of the nearest and second nearest neighbour tree of the same size or larger than the focal tree.

From each tree, we sampled 5 to 10 fully developed leaves from low branches. The leaves sampled from each tree were placed in paper bags. After return from the field, they were dried at 50°C for 30-90 min and then kept on salt until they could be stored at -80°C.

Climate data

Monthly daily mean minimum and maximum temperature values and precipitation data were obtained for the 1 x 1 km grid cells harbouring the sampling sites for the period between 1950 and 2019. Data on the accumulated potential evapotranspiration were obtained for the same grid cells.

265 The data is publicly available from
266 https://opendata.dwd.de/climate_environment/CDC/grids_germany/monthly/.

267 *DNA extraction, construction of GWAS pools and sequencing*

268 DNA was extracted from 12.5 mm² of a single leaf from each tree following the NucleoMag Plant Kit
269 (Macherey Nagel, Düren, Germany) protocol from a total of 196 samples. We set up four DNA pools
270 for poolGWAS: damaged individuals from the Southern part (dSouth), healthy individuals from the
271 South (hSouth), damaged North (dNorth) and healthy North (hNorth). The Southern pools consisted
272 of 100 individuals each, the Northern pools of 50 individuals. The pools were sent to Novogene
273 (Nijmegen, the Netherlands) for library construction and 150bp paired end sequencing with 350bp
274 insert size with 25Gb data for the northern and 38Gb data for the southern samples. The 102
275 individuals used to construct the Northern pools were in addition individually re-sequenced. The
276 exact composition of the genomic pools can be found in Supplemental Table 1.

277 *Reference genome improvement*

278 We used an improved version of the recently published reference genome for the European beech
279 (Mishra *et al.* 2018). Contiguity was improved to chromosome level using Hi-C reads with the help of
280 the allhic software after excluding the probable organelle backbones from the earlier assembly that
281 was generated from the Illumina-corrected PacBio reads using Canu assembler (Mishra et al.,
282 unpublished).

283 *Mapping and variant calling*

284 Reads of pools and individual resequencing were trimmed using the wrapper tool autotrim
285 (Waldvogel *et al.* 2018) that integrates trimmomatic (Bolger *et al.* 2014) for trimming and fastQC
286 (Andrews 2010) for quality control. The trimmed reads were then mapped on the latest chromosome
287 level build of the *F. sylvatica* genome using the BWA mem algorithm (Li & Durbin 2009). Low quality
288 reads were subsequently filtered and SNPs were initially called using samtools (Li *et al.* 2009).

289 *Pool GWAS and PLINK*

290 The PoPoolation pipeline (Kofler *et al.* 2011a; Kofler *et al.* 2011b) was used to call SNPs and remove
291 indels from the four pools. Allele frequencies for all SNPs with a coverage between 15x and 100x with
292 a minimum allele count of three were estimated with the R library PoolSeq (Taus *et al.* 2017).

293 The statistical test to detect significant allele frequency differences among damaged and healthy
294 trees was the Cochran-Mantel-Haenszels test. With this test, a 2x2 table was created for each
295 variable position and region with two phenotypes (healthy and damaged). The read counts of each
296 allele for each phenotype were treated as the dependent variables. We controlled for false discovery
297 rate using the Benjamini-Hochberg correction R package *qvalue* (Dabney *et al.* 2010).

298 For the individual resequencing data we followed the GATK-pipeline 4.1.3.0 (DePristo *et al.* 2011). In
299 short, Picard tools was used to mark duplicates. GVCF files were created with HaplotypeCaller and
300 genotyped with GEnotypeGVCFs. Since we did have a standard SNP set we hard filtered SNPs with
301 VariantFiltration QD<2.0, MQ<50.0, MQRankSum<12.5, ReadPosRankSum<8.0, FS>80.0, SOR>4.0 and
302 QUAL<10.0. This conservative SNP-set was used for base recalibration in the next step, and to run the
303 HaplotypeCaller pipeline a second round. Finally, the genotyped vcf-files were filtered using vcftools
304 with --maf 0.03 --max-missing 0.9 --minQ 25 --min-meanDP 10 --max-meanDP 50 --minDP 10 --
305 maxDP 50.

306 To conduct the GWAS association on the above generated SNP set with phenotypes being either
307 damaged or healthy and to generate a principal component analysis on the SNP positions of the
308 individually resequenced trees, we used PLINK 1.9 (Purcell *et al.* 2007). We calculated a non-
309 parametric ANOSIM on an inter-individual Euclidean distance matrix based on the first ten principal
310 components to infer whether the trees within phenotype groups are overall genetically more similar
311 than within groups (9,999 permutations; (Hammer *et al.* 2001).

312 *Inference of Linkage Disequilibrium*

313 The expected length of segregating haplotypes in a species depends on the recombination rate and
314 their age. The former can be approximated by an estimate of linkage disequilibrium (LD, Feder *et al.*
315 2012). We estimated the extent of LD and its decay using the maximum likelihood method of Feder
316 *et al.* (2012) on one of the pools (healthy South). This method exploits the haplotype information
317 contained in (paired) reads and has been shown to yield accurate estimates if mean LD decay to
318 background levels is shorter than the read length (Feder *et al.* 2012).

319 *Identification substitution type and gene function*

320 We inferred whether significantly differentiated SNPs within genes lead to a (non-) synonymous
321 amino acid substitution using tbg-tools (https://github.com/Croxa/tbg-tools). The protein sequences
322 of the identified genes were used in a blastp search against all non-redundant GenBank CDS
323 translations, PDB, SwissProt, PIR, PRF to infer potential gene functions.

324 *Selection of SNP loci for SNPtype™ assay design*

325 For the design of SNPtype™ assays we used the web-based D3 assay design tool (Fludigm corp.). We
326 aimed in first preference for the most significant SNPs of each genomic region identified by Pool-
327 GWAS (80 loci). If this was technically impossible and the region harboured more than a single
328 significant SNP, we opted for the second most significant SNP and so forth. This resulted finally in 76
329 suitable loci. The remaining 20 loci were recruited from the 20 most significant SNPs of the PLINK
330 analysis that were not scored in the Pool-GWAS.

331 *SNP genotyping procedure*

332 For validation of drought susceptibility associated SNPs, we conducted SNP genotyping on 96.96
333 Dynamic Arrays (Fluidigm) with integrated fluidic circuits (Wang *et al.* 2009). We used the individuals
334 of set 2 (N=53) plus the individuals from set 1 that were not used to construct the GWAS pools
335 (N=42). Prior to the genotyping PCR, DNA extracts were normalised to approximately 5-10 ng/µl.
336 They underwent a pre-amplification PCR (Specific Target Amplification) according to the
337 manufacturer's protocol to enrich target loci. PCR products were diluted 1:10 with DNA suspension
338 buffer (TEKnova, PN T0221) before further use. Genotyping was performed according to the
339 recommendations of the manufacturer. Four additional PCR cycles were added to accommodate for
340 samples of lower quality or including inhibitors {von Thaden, 2020 #45661). Fluorescent data were
341 measured using the EP1 (Fluidigm) and analysed with the SNP Genotyping Analysis Software version
342 4.1.2 (Fluidigm). The automated scoring of the scatter plots was checked visually and if applicable,
343 manually corrected.

344 *Genomic prediction*

345 To predict drought susceptibility from genotype data, we used a linear discriminant analysis (LDA) on
346 92 genotypes scored with the Fluidigm assay at 70 loci. Genotypes homozygous for the reference
347 allele were scored as 0, heterozygous as 1 and homozygous alternate alleles as 2. We arbitrarily

assigned 78 individuals (80%) as training set with known phenotype and used the remaining 15 trees as test set, using the *lda* function of the R package *MASS* (Ripley *et al.* 2013).

Acknowledgments

There was no external funding for this study.

Additional information

Author contributions

Markus Pfenninger: Conceptualisation, sampling, data analysis, writing – original draft. Friederike Reuss, Angelika Kiebler: Laboratory support. Philipp Schönnenfeld, Cosima Caliendo, Susanne Gerber: Bioinformatics support. Berardino Cocchiararo: SNP-assay. Sabrina Reuter, Nico Blüthgen, Carsten Mody: Conceptualisation, sampling, data analysis. Miklós Bálint: Conceptualisation, data analysis. Bagdevi Mishra, Marco Thines: Bioinformatics support. Barbara Feldmeyer: Conceptualisation, labwork, data analysis. All authors read and approved the final version of the manuscript.

Author ORCIDs

Markus Pfenninger 0000-0002-1547-7245

Berardino Cocchiararo 0000-0002-8427-7861

Data availability

All data were made publicly available on ENA (Project Number, pending)

References

Andrews S (2010) FastQC: a quality control tool for high throughput sequence data. Babraham Bioinformatics, Babraham Institute, Cambridge, United Kingdom.

Aranda I, Cano FJ, Gascó A, et al. (2015) Variation in photosynthetic performance and hydraulic architecture across European beech (*Fagus sylvatica* L.) populations supports the case for local adaptation to water stress. *Tree Physiology* **35**, 34-46.

Bastide H, Betancourt A, Nolte V, et al. (2013) A genome-wide, fine-scale map of natural pigmentation variation in *Drosophila melanogaster*. *PLoS Genetics* **9**, e1003534.

Bolger AM, Lohse M, Usadel B (2014) Trimmomatic: a flexible trimmer for Illumina sequence data. *Bioinformatics* **30**, 2114-2120.

Bolte A, Czajkowski T, Cocozza C, et al. (2016) Desiccation and mortality dynamics in seedlings of different European beech (*Fagus sylvatica* L.) populations under extreme drought conditions. *Frontiers in Plant Science* **7**, 751.

Bošeľa M, Sedmák R, Marušák R, et al. (2014) Evaluating similarity of radial increments around tree stem circumference of European beech and Norway spruce from Central Europe. *Geochronometria* **41**, 136-146.

Bressem U (2008) Komplexe Erkrankungen an Buche. [Complex diseases in beech.] *Ergebnisse angewandter Forschung zur Buche* **3**, 87.

Brunet J, Fritz Ö, Richnau G (2010) Biodiversity in European beech forests-a review with recommendations for sustainable forest management. *Ecological Bulletins* **53**, 77-94.

Christensen JH, Hewitson B, Busuioc A, et al. (2007) Regional climate projections. In: Climate Change, 2007: The Physical Science Basis. Contribution of Working group I to the Fourth Assessment Report of

387 the Intergovernmental Panel on Climate Change, University Press, Cambridge, Chapter 11, pp. 847-
388 940.

389 Cocozza C, De Miguel M, Pšidová E, et al. (2016) Variation in ecophysiological traits and drought
390 tolerance of beech (*Fagus sylvatica* L.) seedlings from different populations. *Frontiers in Plant Science*
391 **7**, 886.

392 Czajkowski T, Bolte A (2006) Frosttoleranz deutscher und polnischer Herkünfte der Buche (*Fagus*
393 *sylvatica* L.) und ihre Beeinflussung durch Trockenheit. *Archiv für Forstwesen und*
394 *Landschaftsökologie* **40**, 119-126.

395 Dabney A, Storey JD, Warnes G (2010) qvalue: Q-value estimation for false discovery rate control. R
396 package version 1.

397 DePristo MA, Banks E, Poplin R, et al. (2011) A framework for variation discovery and genotyping
398 using next-generation DNA sequencing data. *Nature Genetics* **43**, 491.

399 Dorow WH, Blick T, Kopelke J-P (2010) Zoologische Forschung in hessischen Naturwaldreservaten–
400 Exemplarische Ergebnisse und Perspektiven. *Forstarchiv* **81**, 61-68.

401 Elsasser P, Meyerhoff J, Weller P (2016) An updated bibliography and database on forest ecosystem
402 service valuation studies in Austria, Germany and Switzerland. *Thünen Working Paper*, Braunschweig.

403 Endler L, Betancourt AJ, Nolte V, Schlötterer C (2016) Reconciling differences in pool-GWAS between
404 populations: a case study of female abdominal pigmentation in *Drosophila melanogaster*. *Genetics*
405 **202**, 843-855.

406 Feder AF, Petrov DA, Bergland AO (2012) LDx: estimation of linkage disequilibrium from high-
407 throughput pooled resequencing data. *PLoS One* **7**, e48588.

408 Gárate-Escamilla H, Hampe A, Vizcaíno-Palomar N, Robson TM, Benito Garzón M (2019) Range-wide
409 variation in local adaptation and phenotypic plasticity of fitness-related traits in *Fagus sylvatica* and
410 their implications under climate change. *Global Ecology and Biogeography* **28**, 1336-1350.

411 Hammer Ø, Harper DA, Ryan PD (2001) PAST: Paleontological statistics software package for
412 education and data analysis. *Palaeontologia Electronica* **4**, 9.

413 Harris K, Nielsen R (2013) Inferring demographic history from a spectrum of shared haplotype
414 lengths. *PLoS Genetics* **9**, e1003521.

415 Harter DE, Nagy L, Backhaus S, et al. (2015) A comparison of genetic diversity and phenotypic
416 plasticity among European beech (*Fagus sylvatica* L.) populations from Bulgaria and Germany under
417 drought and temperature manipulation. *International Journal of Plant Sciences* **176**, 232-244.

418 Hegyi F (1974) A simulation model for managing jack-pine stands. In: Growth models for tree and
419 stand simulation. Fries. J. (ed.), Royal College of Forestry., Stockholm, pp 74–76.

420 Hoban S, Kelley JL, Lotterhos KE, et al. (2016) Finding the genomic basis of local adaptation: pitfalls,
421 practical solutions, and future directions. *The American Naturalist* **188**, 379-397.

422 Kofler R, Orozco-terWengel P, De Maio N, et al. (2011a) PoPoolation: A Toolbox for Population
423 Genetic Analysis of Next Generation Sequencing Data from Pooled Individuals. *PLoS One* **6**, e15925.

424 Kofler R, Pandey RV, Schlötterer C (2011b) PoPoolation2: identifying differentiation between
425 populations using sequencing of pooled DNA samples (Pool-Seq). *Bioinformatics* **27**, 3435-3436.

Kreyling J, Huber G, Jentsch A, et al. (2011) Innerartliche Plastizität und lokale Anpassungen von Waldbäumen. *LWF aktuell* **85**, 12.

Li H, Durbin R (2009) Fast and accurate short read alignment with Burrows-Wheeler Transform. *Bioinformatics* **25**, 1754-1760.

Li H, Handsaker B, Wysoker A, et al. (2009) The Sequence alignment/map (SAM) format and SAMtools. *Bioinformatics* **25**, 2078-2079.

Mishra B, Gupta DK, Pfenninger M, et al. (2018) A reference genome of the European beech (*Fagus sylvatica* L.). *Gigascience* **7**, giy063.

Müller M, Seifert S, Lübbe T, Leuschner C, Finkeldey R (2017) De novo transcriptome assembly and analysis of differential gene expression in response to drought in European beech. *PLoS One* **12**, e0184167.

Müller-Starck G (1985) Genetic differences between" tolerant" and" sensitive" beeches (*Fagus sylvatica* L.) in an environmentally stressed adult forest stand. *Silvae Genetica* **34**, 241-246.

Paar U, Dammann I (2019) Waldzustandsbericht Hessen 2019 (ed. Hessisches Ministerium für Umwelt, Klimaschutz, Landwirtschaft und Verbraucherschutz), Wiesbaden.

Pluess AR, Frank A, Heiri C, et al. (2016) Genome–environment association study suggests local adaptation to climate at the regional scale in *Fagus sylvatica*. *New Phytologist* **210**, 589-601.

Pretzsch H, Schütze G, Uhl E (2013) Resistance of European tree species to drought stress in mixed versus pure forests: evidence of stress release by inter-specific facilitation. *Plant Biology* **15**, 483-495.

Purcell S, Neale B, Todd-Brown K, et al. (2007) PLINK: a tool set for whole-genome association and population-based linkage analyses. *The American Journal of Human Genetics* **81**, 559-575.

Rajendra K, Seifert S, Prinz K, Gailing O, Finkeldey R (2014) Subtle human impacts on neutral genetic diversity and spatial patterns of genetic variation in European beech (*Fagus sylvatica*). *Forest Ecology and Management* **319**, 138-149.

Ripley B, Venables B, Bates DM, et al. (2013) Package 'mass'. Cran R 538.

Schuldt B, Buras A, Arend M, et al. (2020) A first assessment of the impact of the extreme 2018 summer drought on Central European forests. *Basic and Applied Ecology* https://doi.org/10.1016/j.baae.2020.04.003

Stocks JJ, Metheringham CL, Plumb WJ, et al. (2019) Genomic basis of European ash tree resistance to ash dieback fungus. *Nature Ecology & Evolution* **3**, 1686-1696.

Sutmöller J, Spellmann H, Fiebiger C, Albert M (2008) Der Klimawandel und seine Auswirkungen auf die Buchenwälder in Deutschland. [The effects of climate change on beech forests in Germany.] *Ergebnisse angewandter Forschung zur Buche* **3**, 135.

Taus T, Futschik A, Schlötterer C (2017) Quantifying selection with pool-seq time series data. *Molecular Biology and Evolution* **34**, 3023-3034.

Thünen Institute (2020) Clusterstatistik Forst & Holz. Braunschweig.

Trenberth KE, Dai A, Van Der Schrier G, et al. (2014) Global warming and changes in drought. *Nature Climate Change* **4**, 17-22.

von Thaden A., Nowak C, Tiesmeyer A, et al. (2020) Applying genomic data in wildlife monitoring: Development guidelines for genotyping degraded samples with reduced single nucleotide polymorphism panels. *Molecular Ecology Resources* **20,** 662–680.

Waldvogel AM, Feldmeyer B, Rolshausen G, et al. (2020) Evolutionary genomics can improve prediction of species' responses to climate change. *Evolution Letters* **4**, 4-18.

Waldvogel AM, Wieser A, Schell T, et al. (2018) The genomic footprint of climate adaptation in *Chironomus riparius*. *Molecular Ecology* **27**, 1439-1456.

Wang J, Lin M, Crenshaw A, et al. (2009) High-throughput single nucleotide polymorphism genotyping using nanofluidic Dynamic Arrays. *BMC Genomics* **10**, 561.

Wellenreuther M, Hansson B (2016) Detecting polygenic evolution: problems, pitfalls, and promises. *Trends in Genetics* **32**, 155-164.

Figures

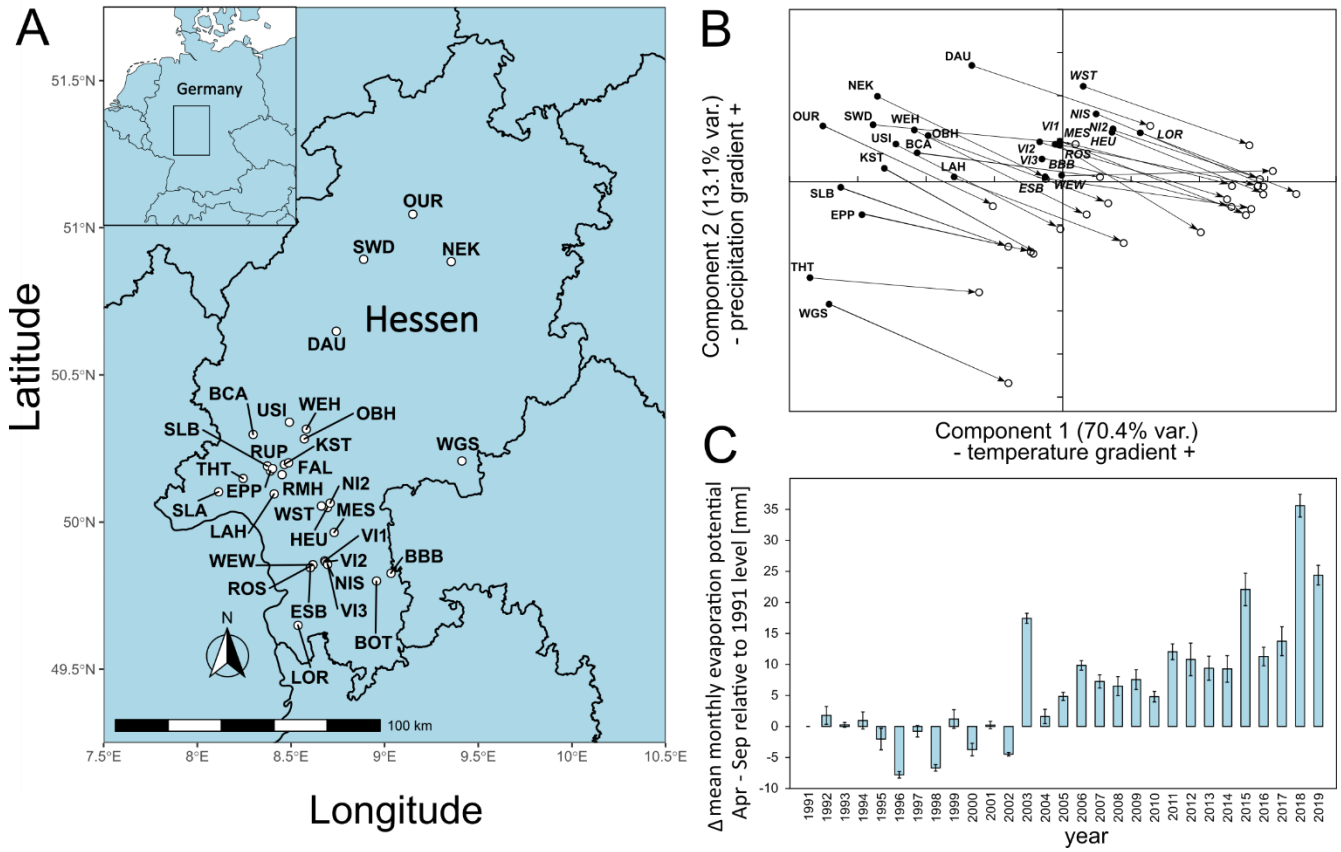

Figure 1. A) Locations of sampling sites in Hessen, Germany. For abbreviations see Suppl. Table 1, B) Principal Component Analysis of monthly climate data 1950-2019, C) Development of main growth period drought indicator from 1991-2019. Shown is the difference mean monthly evaporation potential in mm from April to September relative to the 1991 level. Climate and drought data obtained from https://opendata.dwd.de/climate_environment/CDC/grids_germany/monthly/.

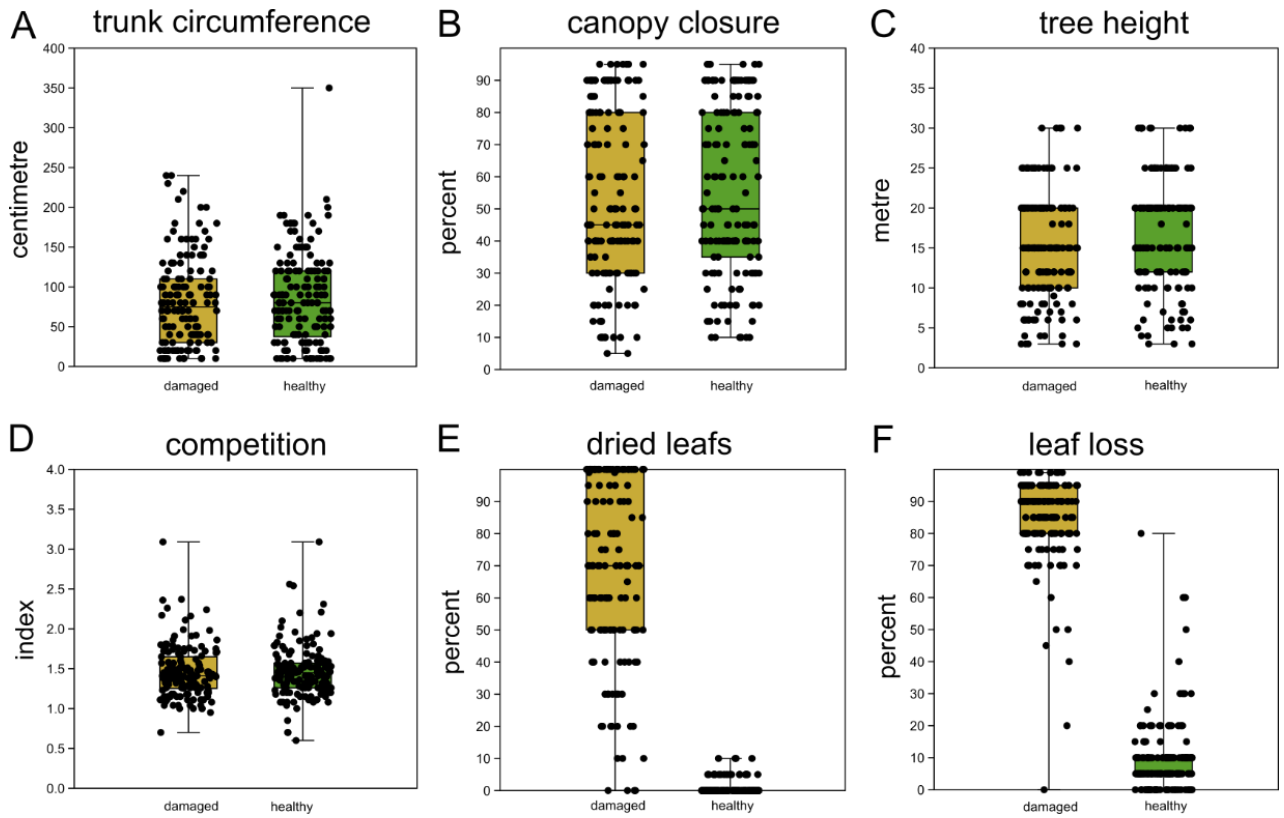

Figure 2. Comparison of sampled beech pairs. A) trunk circumference, B) canopy closure, C) tree height, D) competition index, E) dried leaves and F) leaf loss. Box-plots with indicated means, the boxes represent one standard deviation, the whiskers are the 95% confidence intervals. Damaged trees in ochre, healthy trees in green. Except for E and F, the difference of means among damaged and healthy trees is insignificant between the groups.

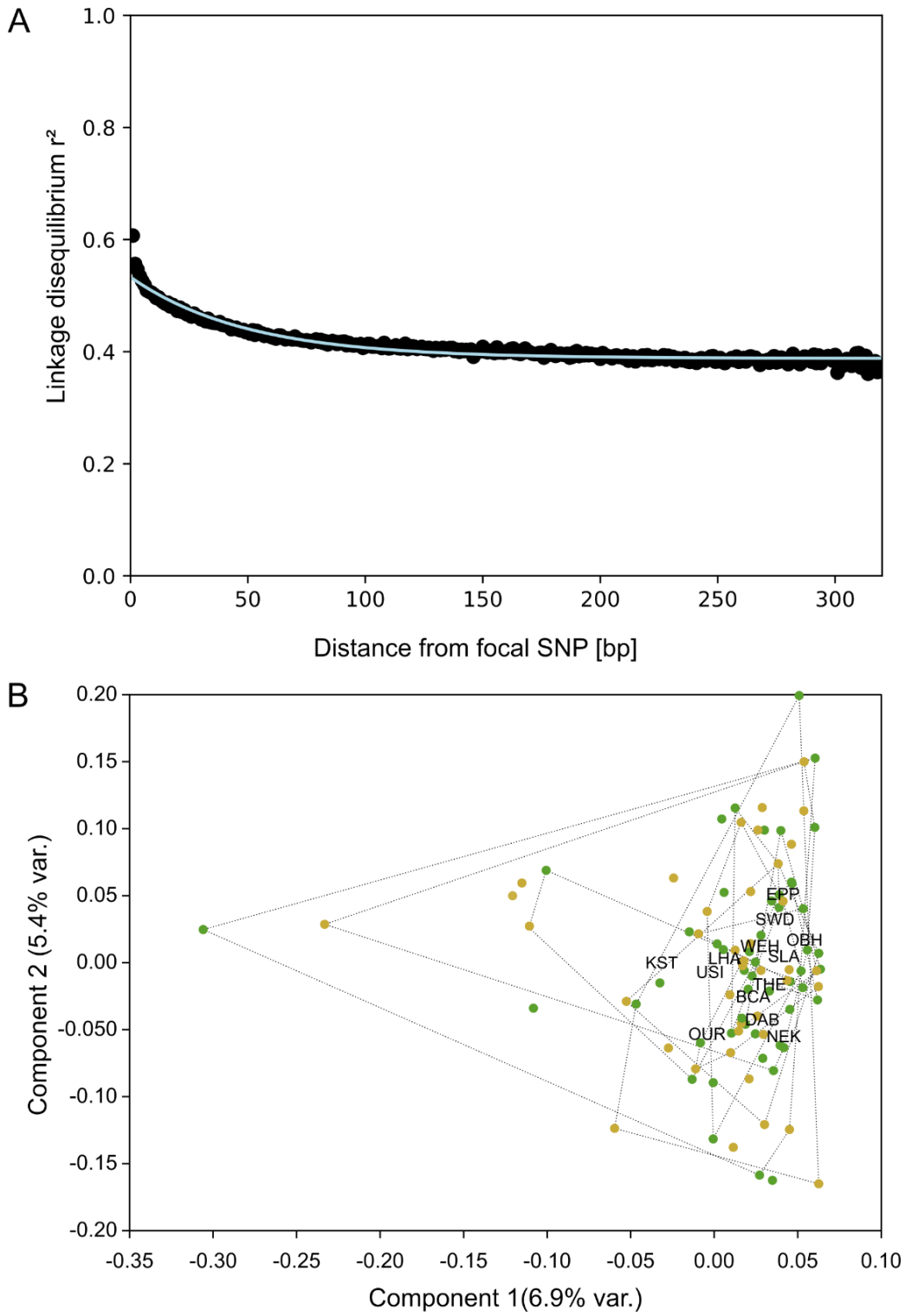

Figure 3. Genome wide linkage disequilibrium and principal component analysis on genome-wide SNP data. A) Decay of genome wide linkage disequilibrium (LD), measured as r^2 on allele frequencies gained from PoolSeq analysis, with distance from focal SNP in base pairs. The blue line represents a fitted exponential decay function. After roughly 100 bp, LD is back to background level. B) Plot of the first two principal component axes of LD pruned SNP data from individually sequenced beech individuals from the North population. Healthy trees are indicated by a green dot, damaged ones by ochre. Individuals sampled from the same site are grouped by convex hulls, limited with dotted lines.

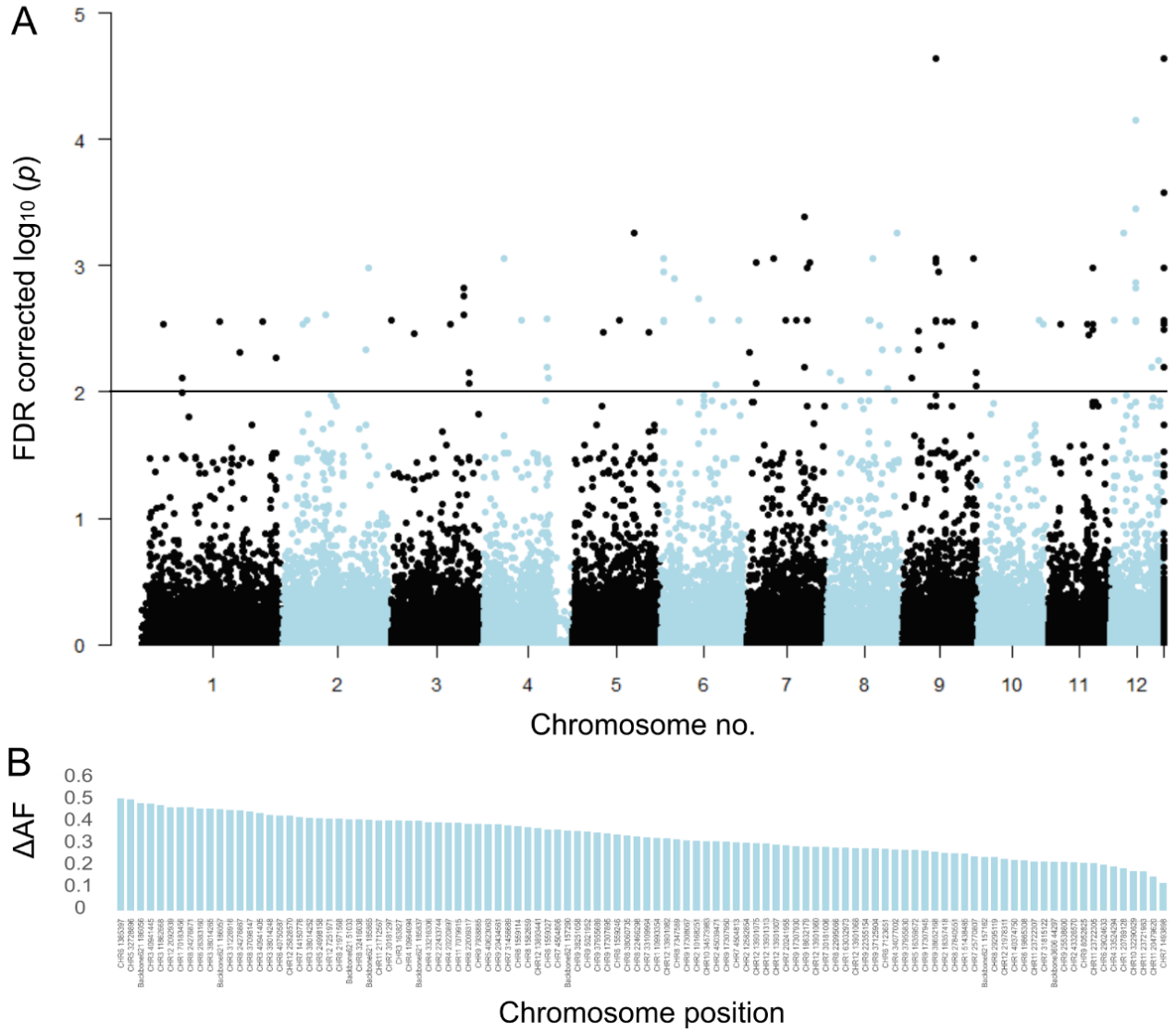

Figure 4. Significantly associated drought phenotype associated SNP marker. A) Manhattan plot of false discovery rate (FDR) corrected –log10 probability values from CMH test. The black horizontal line indicates the chosen significance threshold. SNPs on different chromosomes alternate in colour (black and blue). B) Mean allele frequency difference at significantly associated SNP loci between healthy and damaged phenotypes. The loci are ordered according to amount of change.

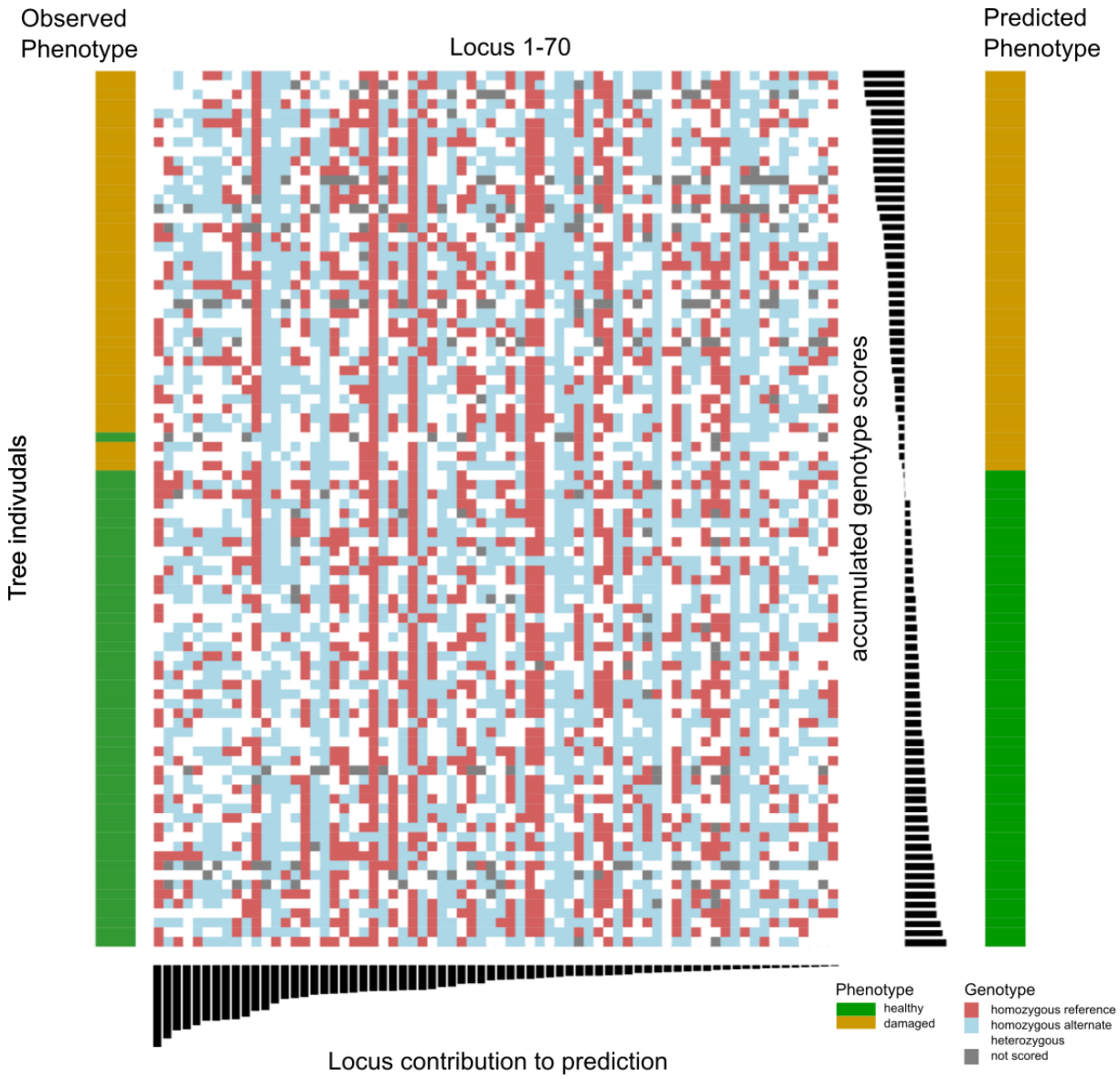

Figure 5. Combined results of SNP assay and discriminant analyses. The centre of the figure depicts the genotypogram of the SNP assay. Each column represents one of 70 loci, each row one of 92 beech individuals. The scored genotypes are colour-coded, with red squares = homozygous reference allele, light blue = homozygous alternate allele, white = heterozygous SNP, grey squares = locus could not be scored in the respective individual. The left bar indicates the observed phenotype for each tree individual with ochre rectangles for damaged, and green for healthy trees. Below the genotypogram, the relative contribution of each locus to the predictive model of the discriminant analysis is indicated, ordered from high to low. On the right side, first the genotype model scores for each individual are given, with the according predicted phenotype (ochre = damaged; green = healthy).

Tables

Key resource table.

Table 1. Genes with significantly associated SNPs. Given are the chromosome number (CHR), nucleotide position (position), the gene ID for *Fagus sylvatica* (gene), the UniProt ID of the closest match (UniProt ID), the name of the gene (name), the nucleotide base in the reference (ref DNA base), and the alternate base (alt DNA base), if applicable, the amino acid of the reference (ref AA) and the alternate base (non-synonymous change), functional change (effect) and the phenotype associated with the alternate base.

CHR	position	gene	UniProt ID	name	ref DNA base	alt DNA base	ref AA	non-synoynmous change	effect	phenotype assoc. with alt base
1	40374762	1.g3851.t1	none		A	G	C	R	SH side chain > positive charge	healthy
10	32290645	10.g3914.t1	none		C	T	F	-	-	
11	20479628	11.g2467.t1	EXOS5_ORYSJ	Exosome complex exonuclease RRP46 homolog	T	C	T	A	polar > hydrophobic	damaged
11	23722307	11.g2832.t1	PCN_ARATH	WD repeat-containing protein PCN	A	G	I	V	hydrophobic > hydrophobic	damaged
12	13901034	12.g1695.t1	F4I5S1_ARATH	PB1 domain-containing protein tyrosine kinase	C	A	P	Q	hydrophobic > polar	damaged
	13901063				C	T	Q	stop	termination	damaged
	13901082				A	T	H	L	positive charge > hydrophobic	damaged
	13901094				T	A	I	N	hydrophobic > polar	damaged
2	43326571	2.g4736.t1	none		G	A	R	C	positive charge > SH side chain	damaged
3	31226940	3.g3590.t1	none		C	T	Q	stop	termination	healthy
4	34077017	4.g3980.t1	CKX1_ARATH	Cytokinin dehydrogenase 1	C	A	G	C	no side chain > SH side chain	damaged
5	16359587	5.g1807.t1	GDI2_ARATH	Guanosine nucleotide diphosphate dissociation inhibitor 2	T	C	P	-	-	
6	19865311	6.g2227.t1	NDUS7_ARATH	NADH dehydrogenase [ubiquinone] iron-sulfur protein 7, mitochondrial	T	C	D	-	-	
6	26383172	6.g2921.t1	none		T	C	A	-	-	
7	1493904	7.g177.t1	TLP10_ARATH	Tubby-like F-box protein 10	C	T	G	-	-	
7	20242023	7.g2350.t1	PRK4_ARATH	Pollen receptor-like kinase 4	A	G	P	-	-	

	4504799				C	T	W	stop	termination	damaged
7	31456694	7.g3617.t1	LSH4_ARATH	Protein LIGHT-DEPENDENT SHORT HYPOCOTYLS 4	G	T	R	-	-	
7	33110000	7.g3816.t1	none		G	A	L	-	-	
7	4504813	7.g552.t1	none		G	A	G	-	-	
	4504831				C	T	L	-	-	
8	29295139	8.g3494.t1	VATC_ARATH	V-type proton ATPase subunit C	G	A	G	-	-	
9	25538827	9.g3080.t1	PPA14_ARATH	Probable inactive purple acid phosphatase 14	G	C	K	N	positive charge > polar	damaged
9	37955715	9.g4504.t1	TBL33_ARATH	Protein trichome birefringence-like 33	G	C	M	I	hydrophobic > hydrophobic	damaged

Supplemental Material

Suppl. Table 1. Sampled *Fagus sylvatica* individuals. Given are the phenotype, sampling location, sampling date, geographical coordinates in decimal degrees, the pool to which the individual contributed, whether it was individually re-sequenced (x) and whether it was used in the SNP assay to validate the results (x).

TreeID	Phenotype	Location	Sampling date	Latitude	Longitude	Pool (set 1)	individually re-sequenced	Validation (set 2)
PF_001	damaged	Königstein	29.08.2019	50.1957342	8.4648591	dNorth		
PF_002	healthy	Königstein	29.08.2019	50.1957187	8.4648341	hNorth	x	
PF_003	damaged	Königstein	29.08.2019	50.1964726	8.4664262	dNorth	x	
PF_004	healthy	Königstein	29.08.2019	50.1964232	8.4664275	hNorth	x	
PF_005	damaged	Königstein	29.08.2019	50.1929421	8.456941	dNorth	x	
PF_006	healthy	Königstein	29.08.2019	50.1928331	8.4568086	hNorth	x	
PF_007	damaged	Königstein	29.08.2019	50.1925453	8.457816	dNorth	x	
PF_008	healthy	Königstein	29.08.2019	50.1925741	8.4578839	hNorth	x	
PF_009	damaged	Königstein	29.08.2019	50.1926029	8.4579518	dNorth	x	
PF_010	healthy	Königstein	29.08.2019	50.1926317	8.4580197	hNorth	x	
PF_011	damaged	Obernhain	03.09.2019	50.2825898	8.5712681	dNorth		
PF_012	healthy	Obernhain	03.09.2019	50.2827911	8.5711075	hNorth		
PF_013	damaged	Obernhain	03.09.2019	50.2820637	8.5734056	dNorth		
PF_014	healthy	Obernhain	03.09.2019	50.282214	8.5734601	hNorth		
PF_015	damaged	Obernhain	03.09.2019	50.2817116	8.5761923	dNorth		
PF_016	healthy	Obernhain	03.09.2019	50.2816381	8.5761487	hNorth	x	
PF_017	damaged	Obernhain	03.09.2019	50.2821782	8.5704083	dNorth	x	
PF_018	healthy	Obernhain	03.09.2019	50.2821327	8.5704883	hNorth	x	
PF_019	damaged	Obernhain	03.09.2019	50.2816941	8.5700475	dNorth	x	
PF_020	healthy	Obernhain	03.09.2019	50.2817058	8.570133	hNorth	x	
PF_021	damaged	Usingen	04.09.2019	50.3392732	8.4913495	dNorth	x	
PF_022	healthy	Usingen	04.09.2019	50.3391762	8.491312	hNorth	x	
PF_023	damaged	Usingen	04.09.2019	50.3397337	8.4924001	dNorth	x	
PF_024	healthy	Usingen	04.09.2019	50.3396942	8.4924593	hNorth	x	
PF_025	damaged	Usingen	04.09.2019	50.344079	8.4932305	dNorth	x	
PF_026	healthy	Usingen	04.09.2019	50.3440912	8.4933098	hNorth	x	
PF_027	damaged	Usingen	04.09.2019	50.3452681	8.4959808	dNorth	x	
PF_028	healthy	Usingen	04.09.2019	50.3451246	8.4962431	hNorth	x	
PF_029	damaged	Usingen	04.09.2019	50.3416761	8.4918323	dNorth	x	
PF_030	healthy	Usingen	04.09.2019	50.3417203	8.4917173	hNorth	x	
PF_031	damaged	Eppenhain	05.09.2019	50.1736813	8.3908577	dNorth	x	
PF_032	healthy	Eppenhain	05.09.2019	50.1736578	8.39113553	hNorth	x	
PF_033	damaged	Eppenhain	05.09.2019	50.1750866	8.3891472	dNorth	x	
PF_034	healthy	Eppenhain	05.09.2019	50.175069	8.3892187	hNorth	x	
PF_035	damaged	Eppenhain	05.09.2019	50.1754443	8.3876407	dNorth	x	
PF_036	healthy	Eppenhain	05.09.2019	50.1754007	8.3875849	hNorth	x	
PF_037	damaged	Eppenhain	05.09.2019	50.1746449	8.3872509	dNorth	x	
PF_038	healthy	Eppenhain	05.09.2019	50.1746095	8.3874874	hNorth	x	
PF_039	damaged	Eppenhain	05.09.2019	50.1734334	8.3904983	dNorth	x	
PF_040	healthy	Eppenhain	05.09.2019	50.1733173	8.390211	hNorth	x	
PF_041	damaged	Eppenhain	05.09.2019	50.1745915	8.3907433	dNorth	x	
PF_042	healthy	Eppenhain	05.09.2019	50.1745128	8.3908124	hNorth	x	
PF_050	damaged	Bad Camberg	06.09.2019	50.2976336	8.2980473	dNorth		
PF_051	healthy	Bad Camberg	06.09.2019	50.2975811	8.298169	hNorth		
PF_052	damaged	Daubringen	07.09.2019	50.6483759	8.7419719	dNorth	x	
PF_053	healthy	Daubringen	07.09.2019	50.6482664	8.7421457	hNorth	x	
PF_054	damaged	Daubringen	07.09.2019	50.6480228	8.7428739	dNorth	x	
PF_055	healthy	Daubringen	07.09.2019	50.6478157	8.742954	hNorth	x	
PF_056	damaged	Daubringen	07.09.2019	50.648846	8.7426283	dNorth	x	
PF_057	healthy	Daubringen	07.09.2019	50.6489798	8.7423211	hNorth	x	
PF_058	damaged	Schwabendorf	07.09.2019	50.8927904	8.8879419	dNorth	x	
PF_059	healthy	Schwabendorf	07.09.2019	50.8929008	8.8881284	hNorth	x	
PF_060	damaged	Schwabendorf	07.09.2019	50.8951542	8.8822243	dNorth	x	
PF_061	healthy	Schwabendorf	07.09.2019	50.8952005	8.882144	hNorth	x	
PF_062	damaged	Oberurff	07.09.2019	51.0458016	9.1505195	dNorth	x	
PF_063	healthy	Oberurff	07.09.2019	51.0457499	9.1505234	hNorth	x	
PF_064	damaged	Oberurff	07.09.2019	51.0461483	9.1478112	dNorth	x	

PF_065	healthy	Oberurff	07.09.2019	51.0461706	9.1474544	hNorth	x	
PF_066	damaged	Oberurff	07.09.2019	51.0453396	9.1466057	dNorth	x	
PF_067	healthy	Oberurff	07.09.2019	51.0453396	9.146057	hNorth	x	
PF_068	damaged	Oberurff	07.09.2019	51.0463978	9.1432389	dNorth	x	
PF_069	healthy	Oberurff	07.09.2019	51.0464672	9.1435546	hNorth	x	
PF_070	damaged	Neukirchen	08.09.2019	50.8848091	9.3557289	dNorth	x	
PF_071	healthy	Neukirchen	08.09.2019	50.88496	9.3560291	hNorth	x	
PF_072	damaged	Langenhain	09.09.2019	50.0955818	8.4101217	dNorth	x	
PF_073	healthy	Langenhain	09.09.2019	50.0956666	8.4105235	hNorth	x	
PF_074	damaged	Langenhain	09.09.2019	50.0959896	8.4104922	dNorth	x	
PF_075	healthy	Langenhain	09.09.2019	50.0960509	8.4105981	hNorth	x	
PF_076	damaged	Langenhain	09.09.2019	50.0947953	8.4151317	dNorth	x	
PF_077	healthy	Langenhain	09.09.2019	50.0947434	8.4150994	hNorth	x	
PF_078	damaged	Langenhain	09.09.2019	50.0911467	8.41578726	dNorth	x	
PF_079	healthy	Langenhain	09.09.2019	50.0912627	8.415817	hNorth		
PF_080	damaged	Langenhain	09.09.2019	50.0901299	8.4166724	dNorth	x	
PF_081	healthy	Langenhain	09.09.2019	50.090096	8.4166748	hNorth	x	
PF_082	damaged	Langenhain	09.09.2019	50.0940815	8.4100466	dNorth	x	
PF_083	healthy	Langenhain	09.09.2019	50.0939183	8.4099548	hNorth	x	
PF_085	damaged	Theistal	11.09.2019	50.1480865	8.2445088	dNorth	x	
PF_086	healthy	Theistal	11.09.2019	50.1480164	8.2447881	hNorth	x	
PF_087	damaged	Theistal	11.09.2019	50.1517267	8.2464193	dNorth	x	
PF_088	healthy	Theistal	11.09.2019	50.151875	8.2461256	hNorth	x	
PF_089	damaged	Theistal	11.09.2019	50.1532534	8.2456221	dNorth	x	
PF_090	healthy	Theistal	11.09.2019	50.1528409	8.2455616	hNorth	x	
PF_091	damaged	Theistal	11.09.2019	50.1539513	8.2466804	dNorth	x	
PF_092	healthy	Theistal	11.09.2019	50.1540134	8.2462949	hNorth	x	
PF_093	damaged	Schlangenbad	11.09.2019	50.1027276	8.1136673	dNorth	x	
PF_094	healthy	Schlangenbad	11.09.2019	50.1025753	8.1136931	hNorth	x	
PF_095	damaged	Schlangenbad	11.09.2019	50.0997272	8.1101568	dNorth	x	
PF_096	healthy	Schlangenbad	11.09.2019	50.099823	8.1103387	hNorth	x	
PF_100	damaged	Wehrheim	12.09.2019	50.3153263	8.5819508	dNorth	x	
PF_101	healthy	Wehrheim	12.09.2019	50.315372	8.5820711	hNorth	x	
PF_102	damaged	Wehrheim	12.09.2019	50.3145513	8.5854558	dNorth	x	
PF_103	healthy	Wehrheim	12.09.2019	50.3145748	8.585572	hNorth	x	
PF_104	damaged	Wehrheim	12.09.2019	50.3147404	8.585804	dNorth	x	
PF_105	healthy	Wehrheim	12.09.2019	50.3146745	8.5858773	hNorth	x	
PF_106	damaged	Wehrheim	12.09.2019	50.3149149	8.5859893	dNorth	x	
PF_107	healthy	Wehrheim	12.09.2019	50.31472242	8.5861579	hNorth	x	
PF_108	damaged	Wehrheim	12.09.2019	50.3149559	8.5866045	dNorth	x	
PF_109	healthy	Wehrheim	12.09.2019	50.3150733	8.5866527	hNorth	x	
PF_110	damaged	Wehrheim	12.09.2019	50.3155392	8.587186	dNorth	x	
PF_111	healthy	Wehrheim	12.09.2019	50.3154613	8.5872255	hNorth	x	
PF_112	damaged	Wehrheim	12.09.2019	50.3130127	8.580265	dNorth	x	
PF_113	healthy	Wehrheim	12.09.2019	50.3130103	8.5800785	hNorth	x	
PF_114	damaged	Wehrheim	12.09.2019	50.3141899	8.581059	dNorth	x	
PF_115	healthy	Wehrheim	12.09.2019	50.314164	8.5809636	hNorth	x	
S_001	damaged	Bot. Garten	26.08.2019	49.79971	8.95682	dSouth		
S_002	healthy	Bot. Garten	26.08.2019	49.86852	8.67999	hSouth		
S_003	damaged	Bot. Garten	26.08.2019	49.86856	8.68018	dSouth		
S_004	healthy	Bot. Garten	26.08.2019	49.86856	8.68018	hSouth		
S_005	damaged	Vivarium	26.08.2019	49.86855	8.68017	dSouth		
S_006	healthy	Vivarium	26.08.2019	49.86436	8.6842	hSouth		
S_007	damaged	Vivarium	26.08.2019	49.8644	8.68418	dSouth		
S_008	healthy	Vivarium	26.08.2019	49.8644	8.68418	hSouth		
S_009	damaged	Vivarium	26.08.2019	49.8644	8.68418	dSouth		
S_010	healthy	Vivarium	26.08.2019	49.8644	8.68418	hSouth		
S_011	damaged	Vivarium	26.08.2019	49.8644	8.68418	dSouth		
S_012	healthy	Vivarium	26.08.2019	49.8644	8.68418	hSouth		
S_013	damaged	VivariumII	26.08.2019	49.8644	8.68418	dSouth		
S_014	healthy	VivariumII	26.08.2019	49.8644	8.68418	hSouth		
S_015	damaged	VivariumII	26.08.2019	49.86227	8.68876	dSouth		
S_016	healthy	VivariumII	26.08.2019	49.86241	8.68874	hSouth		
S_017	damaged	VivariumII	26.08.2019	49.86199	8.68894	dSouth		
S_018	healthy	VivariumII	26.08.2019	49.86196	8.68885	hSouth		
S_019	damaged	VivariumII	26.08.2019	49.86092	8.69278	dSouth		
S_020	healthy	VivariumII	26.08.2019	49.86031	8.69225	hSouth		
S_021	damaged	VivariumIII	27.08.2019	49.85883	8.69445	dSouth		

S_022	healthy	VivariumIII	27.08.2019	49.85883	8.69445	hSouth		
S_023	damaged	VivariumIII	27.08.2019	49.85882	8.69446	dSouth		
S_024	healthy	VivariumIII	27.08.2019	49.85882	8.69446	hSouth		
S_025	damaged	VivariumIII	27.08.2019	49.85862	8.6944	dSouth		
S_026	healthy	VivariumIII	27.08.2019	49.85862	8.6944	hSouth		
S_027	damaged	VivariumIII	27.08.2019	49.85637	8.69584	dSouth		
S_028	healthy	VivariumIII	27.08.2019	49.85637	8.69584	hSouth		
S_029	damaged	VivariumIII	27.08.2019	49.8565	8.69616	dSouth		
S_030	healthy	VivariumIII	27.08.2019	49.8565	8.69616	hSouth		
S_031	damaged	VivariumIII	27.08.2019	49.8565	8.69616	dSouth		
S_032	healthy	VivariumIII	27.08.2019	49.8565	8.69616	hSouth		
S_033	damaged	VivariumIII	27.08.2019	49.85576	8.69886	dSouth		
S_034	healthy	VivariumIII	27.08.2019	49.85576	8.69886	hSouth		
S_035	damaged	VivariumIII	27.08.2019	49.85576	8.69886	dSouth		
S_036	healthy	VivariumIII	27.08.2019	49.85576	8.69886	hSouth		
S_037	damaged	VivariumIII	27.08.2019	49.85329	8.6938	dSouth		
S_038	healthy	VivariumIII	27.08.2019	49.85329	8.6938	hSouth		
S_039	damaged	VivariumIII	27.08.2019	49.85329	8.6938	dSouth		
S_040	healthy	VivariumIII	27.08.2019	49.85329	8.6938	hSouth		
S_041	damaged	VivariumIII	27.08.2019	49.85021	8.9391	dSouth		
S_042	healthy	VivariumIII	27.08.2019	49.85021	8.9391	hSouth		
S_043	damaged	Neu-Isenburg	28.08.2019	49.85585	8.69554	dSouth		
S_044	healthy	Neu-Isenburg	28.08.2019	49.85585	8.69554	hSouth		
S_045	damaged	Neu-Isenburg	28.08.2019	49.85585	8.69554	dSouth		
S_046	healthy	Neu-Isenburg	28.08.2019	49.85585	8.69554	hSouth		
S_047	damaged	Neu-Isenburg	28.08.2019	49.85585	8.69554	dSouth		
S_048	healthy	Neu-Isenburg	28.08.2019	49.85585	8.69554	hSouth		
S_049	damaged	Neu-Isenburg	28.08.2019	49.85585	8.69554	dSouth		
S_050	healthy	Neu-Isenburg	28.08.2019	49.85585	8.69554	hSouth		
S_051	damaged	Neu-Isenburg	28.08.2019	49.85585	8.69554	dSouth		
S_052	healthy	Neu-Isenburg	28.08.2019	49.85585	8.69554	hSouth		
S_053	damaged	Neu-Isenburg	28.08.2019	49.85585	8.69554	dSouth		
S_054	healthy	Neu-Isenburg	28.08.2019	49.85585	8.69554	hSouth		
S_055	damaged	Neu-Isenburg	28.08.2019	49.85585	8.69554	dSouth		
S_056	healthy	Neu-Isenburg	28.08.2019	49.85585	8.69554	hSouth		
S_057	damaged	Neu-Isenburg	28.08.2019	49.85585	8.69554	dSouth		
S_058	healthy	Neu-Isenburg	28.08.2019	49.85585	8.69554	hSouth		
S_059	damaged	Neu-Isenburg	28.08.2019	49.85585	8.69554	dSouth		
S_060	healthy	Neu-Isenburg	28.08.2019	49.85585	8.69554	hSouth		
S_061	damaged	Westwald	29.09.2019	49.855069	8.617017	dSouth		
S_062	healthy	Westwald	29.09.2019	49.855069	8.617017	hSouth		
S_063	damaged	Westwald	29.09.2019	49.85495	8.61703	dSouth		
S_064	healthy	Westwald	29.09.2019	49.85495	8.61703	hSouth		
S_065	damaged	Westwald	29.09.2019	49.85495	8.61703	dSouth		
S_066	healthy	Westwald	29.09.2019	49.85495	8.61703	hSouth		
S_067	damaged	Westwald	29.09.2019	49.85494	8.61702	dSouth		
S_068	healthy	Westwald	29.09.2019	49.85494	8.61702	hSouth		
S_069	damaged	Westwald	29.09.2019	49.854909	8.618146	dSouth		
S_070	healthy	Westwald	29.09.2019	49.854909	8.618146	hSouth		
S_071	damaged	Westwald	29.09.2019	49.85494	8.61702	dSouth		
S_072	healthy	Westwald	29.09.2019	49.85494	8.61702	hSouth		
S_073	damaged	Westwald	29.09.2019	49.85494	8.61702	dSouth		
S_074	healthy	Westwald	29.09.2019	49.85494	8.61702	hSouth		
S_075	damaged	Westwald	29.09.2019	49.85494	8.61702	dSouth		
S_076	healthy	Westwald	29.09.2019	49.85494	8.61702	hSouth		
S_077	damaged	Westwald	29.09.2019	49.85494	8.61702	dSouth		
S_078	healthy	Westwald	29.09.2019	49.85494	8.61702	hSouth		
S_079	damaged	Westwald	29.09.2019	49.85494	8.61702	dSouth		
S_080	healthy	Westwald	29.09.2019	49.85494	8.61702	hSouth		
S_081	damaged	Westwald	29.09.2019	49.85494	8.61702	dSouth		
S_082	healthy	Westwald	29.09.2019	49.85494	8.61702	hSouth		
S_083	damaged	Westwald	29.09.2019	49.85494	8.61702	dSouth		
S_084	healthy	Westwald	29.09.2019	49.85494	8.61702	hSouth		
S_085	damaged	Roßdorf	02.09.2019	49.85494	8.61702	dSouth		
S_086	healthy	Roßdorf	02.09.2019	49.85494	8.61702	hSouth		
S_087	damaged	Roßdorf	02.09.2019	49.85943	8.70791	dSouth		
S_088	healthy	Roßdorf	02.09.2019	49.85943	8.70791	hSouth		
S_089	damaged	Roßdorf	02.09.2019	49.85943	8.70786	dSouth		

S_090	healthy	Roßdorf	02.09.2019	49.85943	8.70786	hSouth		
S_091	damaged	Roßdorf	02.09.2019	49.85977	8.70795	dSouth		
S_092	healthy	Roßdorf	02.09.2019	49.85977	8.70795	hSouth		
S_093	damaged	Roßdorf	02.09.2019	49.86221	8.718	dSouth		
S_094	healthy	Roßdorf	02.09.2019	49.86221	8.718	hSouth		
S_095	damaged	Roßdorf	02.09.2019	49.86211	8.71801	dSouth		
S_096	healthy	Roßdorf	02.09.2019	49.86211	8.71801	hSouth		
S_097	damaged	Roßdorf	02.09.2019	49.86211	8.71801	dSouth		
S_098	healthy	Roßdorf	02.09.2019	49.86211	8.71801	hSouth		
S_099	damaged	Roßdorf	02.09.2019	49.86089	8.70835	dSouth		
S_100	healthy	Roßdorf	02.09.2019	49.86089	8.70835	hSouth		
S_101	damaged	Roßdorf	02.09.2019	49.86095	8.70771	dSouth		
S_102	healthy	Roßdorf	02.09.2019	49.86095	8.70771	hSouth		
S_103	damaged	Roßdorf	02.09.2019	49.86103	8.70769			x
S_104	healthy	Roßdorf	02.09.2019	49.86103	8.70769			x
S_105	damaged	Burg Breuberg	03.09.2019	49.8259	9.0341	dSouth		
S_106	healthy	Burg Breuberg	03.09.2019	49.8259	9.0341	hSouth		
S_107	damaged	Burg Breuberg	03.09.2019	49.82447	9.03196	dSouth		
S_108	healthy	Burg Breuberg	03.09.2019	49.82447	9.03196	hSouth		
S_109	damaged	Burg Breuberg	03.09.2019	49.82457	9.03155	dSouth		
S_110	healthy	Burg Breuberg	03.09.2019	49.82457	9.03155	hSouth		
S_111	damaged	Burg Breuberg	03.09.2019	49.82736	9.0267	dSouth		
S_112	healthy	Burg Breuberg	03.09.2019	49.82736	9.0267	hSouth		
S_113	damaged	Burg Breuberg	03.09.2019	49.827	9.02706	dSouth		
S_114	healthy	Burg Breuberg	03.09.2019	49.827	9.02706	hSouth		
S_115	damaged	Burg Breuberg	03.09.2019	49.82689	9.02076	dSouth		
S_116	healthy	Burg Breuberg	03.09.2019	49.82689	9.02076	hSouth		
S_117	damaged	Burg Breuberg	03.09.2019	49.82692	9.02038			x
S_118	healthy	Burg Breuberg	03.09.2019	49.82692	9.02038			x
S_119	damaged	Burg Breuberg	03.09.2019	49.82322	9.02107	dSouth		
S_120	healthy	Burg Breuberg	03.09.2019	49.82322	9.02107	hSouth		
S_121	damaged	Burg Breuberg	03.09.2019	49.82305	9.02048	dSouth		
S_122	healthy	Burg Breuberg	03.09.2019	49.82305	9.02048	hSouth		
S_123	damaged	Burg Breuberg	03.09.2019	49.82301	9.02096	dSouth		
S_124	healthy	Burg Breuberg	03.09.2019	49.82301	9.02096	hSouth		
S_125	damaged	Heusenstamm	04.09.2019	50.04919	8.69445	dSouth		
S_126	healthy	Heusenstamm	04.09.2019	50.04919	8.69445	hSouth		
S_127	damaged	Heusenstamm	04.09.2019	50.04919	8.69445	dSouth		
S_128	healthy	Heusenstamm	04.09.2019	50.04919	8.69445	hSouth		
S_129	damaged	Heusenstamm	04.09.2019	50.0577	8.7788			x
S_130	healthy	Heusenstamm	04.09.2019	50.0577	8.7788			x
S_131	damaged	Heusenstamm	04.09.2019	50.0575	8.7787	dSouth		
S_132	healthy	Heusenstamm	04.09.2019	50.0575	8.7787	hSouth		
S_133	damaged	Heusenstamm	04.09.2019	50.05774	8.7796	dSouth		
S_134	healthy	Heusenstamm	04.09.2019	50.05774	8.7796	hSouth		
S_135	damaged	Heusenstamm	04.09.2019	50.05574	8.7795	dSouth		
S_136	healthy	Heusenstamm	04.09.2019	50.05574	8.7795	hSouth		
S_137	damaged	Heusenstamm	04.09.2019	50.0562	8.7787	dSouth		
S_138	healthy	Heusenstamm	04.09.2019	50.0562	8.7787	hSouth		
S_139	damaged	Heusenstamm	04.09.2019	50.0562	8.7787	dSouth		
S_140	healthy	Heusenstamm	04.09.2019	50.0562	8.7787	hSouth		
S_141	damaged	Heusenstamm	04.09.2019	50.0562	8.7787	dSouth		
S_142	healthy	Heusenstamm	04.09.2019	50.0562	8.7787	hSouth		
S_143	damaged	Heusenstamm	04.09.2019	50.0562	8.7787			x
S_144	healthy	Heusenstamm	04.09.2019	50.0562	8.7787			x
S_145	damaged	Heusenstamm	04.09.2019	50.0556	8.7788			x
S_146	healthy	Heusenstamm	04.09.2019	50.0556	8.7788			x
S_147	damaged	Heusenstamm	04.09.2019	50.056	8.78	dSouth		
S_148	healthy	Heusenstamm	04.09.2019	50.056	8.78	hSouth		
S_149	damaged	Heusenstamm	04.09.2019	50.0557	8.779	dSouth		
S_150	healthy	Heusenstamm	04.09.2019	50.0557	8.779	hSouth		
S_151	damaged	Heusenstamm	04.09.2019	50.0557	8.779	dSouth		
S_152	healthy	Heusenstamm	04.09.2019	50.0557	8.779	hSouth		
S_153	damaged	Heusenstamm	04.09.2019	50.0552	8.7797	dSouth		
S_154	healthy	Heusenstamm	04.09.2019	50.0552	8.7797	hSouth		
S_155	damaged	Eschollbrücken	06.09.2019	49.844862	8.6033987	dSouth		
S_156	healthy	Eschollbrücken	06.09.2019	49.844862	8.6033987	hSouth		
S_157	damaged	Eschollbrücken	06.09.2019	49.8451033	8.6033906	dSouth		

S_158	healthy	Eschollbrücken	06.09.2019	49.8451033	8.6033906	hSouth		
S_159	damaged	Eschollbrücken	06.09.2019	49.8452741	8.6933477	dSouth		
S_160	healthy	Eschollbrücken	06.09.2019	49.8452741	8.6933477	hSouth		
S_161	damaged	Eschollbrücken	06.09.2019	49.8464188	8.6058807	dSouth		
S_162	healthy	Eschollbrücken	06.09.2019	49.8464188	8.6058807	hSouth		
S_163	damaged	Eschollbrücken	06.09.2019	49.8461255	8.6064631			x
S_164	healthy	Eschollbrücken	06.09.2019	49.8461255	8.6064631			x
S_165	damaged	Eschollbrücken	06.09.2019	49.8381468	8.613406	dSouth		
S_166	healthy	Eschollbrücken	06.09.2019	49.8381468	8.613406	hSouth		
S_167	damaged	Eschollbrücken	06.09.2019	49.8371837	8.6154874	dSouth		
S_168	healthy	Eschollbrücken	06.09.2019	49.8371837	8.6154874	hSouth		
S_169	damaged	Eschollbrücken	06.09.2019	49.8368364	8.6172492			x
S_170	healthy	Eschollbrücken	06.09.2019	49.8368364	8.6172492			x
S_171	damaged	Eschollbrücken	06.09.2019	49.8364971	8.6193427	dSouth		
S_172	healthy	Eschollbrücken	06.09.2019	49.8364971	8.6193427	hSouth		
S_173	damaged	Eschollbrücken	06.09.2019	49.8366439	8.617927	dSouth		
S_174	healthy	Eschollbrücken	06.09.2019	49.8366439	8.617927	hSouth		
S_175	damaged	Eschollbrücken	06.09.2019	49.83549	8.6063276			x
S_176	healthy	Eschollbrücken	06.09.2019	49.83549	8.6063276			x
S_177	damaged	Eschollbrücken	06.09.2019	49.836002	8.6057516	dSouth		
S_178	healthy	Eschollbrücken	06.09.2019	49.836002	8.6057516	hSouth		
S_179	damaged	Eschollbrücken	06.09.2019	49.8364465	8.6051897			x
S_180	healthy	Eschollbrücken	06.09.2019	49.8364465	8.6051897			x
S_181	damaged	Neu Isenburg	09.09.2019	50.0643187	8.7090884	dSouth		
S_182	healthy	Neu Isenburg	09.09.2019	50.0643187	8.7090884	hSouth		
S_183	damaged	Neu Isenburg	09.09.2019	50.0650797	8.7098096	dSouth		
S_184	healthy	Neu Isenburg	09.09.2019	50.0650797	8.7098096	hSouth		
S_185	damaged	Neu Isenburg	09.09.2019	50.0659154	8.7102773	dSouth		
S_186	healthy	Neu Isenburg	09.09.2019	50.0659154	8.7102773	hSouth		
S_187	damaged	Neu Isenburg	09.09.2019	50.0659301	8.7100359	dSouth		
S_188	healthy	Neu Isenburg	09.09.2019	50.0659301	8.7100359	hSouth		
S_189	damaged	Neu Isenburg	09.09.2019	50.0686111	8.7121451	dSouth		
S_190	healthy	Neu Isenburg	09.09.2019	50.0686111	8.7121451	hSouth		
S_191	damaged	Neu Isenburg	09.09.2019	50.0691756	8.7123064	dSouth		
S_192	healthy	Neu Isenburg	09.09.2019	50.0691756	8.7123064	hSouth		
S_193	damaged	Neu Isenburg	09.09.2019	50.0710306	8.7127781	dSouth		
S_194	healthy	Neu Isenburg	09.09.2019	50.0710306	8.7127781	hSouth		
S_195	damaged	Neu Isenburg	09.09.2019	50.0716691	8.7111252	dSouth		
S_196	healthy	Neu Isenburg	09.09.2019	50.0716691	8.7111252	hSouth		
S_197	damaged	Neu Isenburg	09.09.2019	50.0715402	8.7110297	dSouth		
S_198	healthy	Neu Isenburg	09.09.2019	50.0715402	8.7110297	hSouth		
S_199	damaged	Neu Isenburg	09.09.2019	50.0710603	8.7121176	dSouth		
S_200	healthy	Neu Isenburg	09.09.2019	50.0710603	8.7121176	hSouth		
S_201	damaged	Neu Isenburg	09.09.2019	50.0681943	8.7052592	dSouth		
S_202	healthy	Neu Isenburg	09.09.2019	50.0681943	8.7052592	hSouth		
S_203	damaged	Neu Isenburg	09.09.2019	50.0671452	8.7042427	dSouth		
S_204	healthy	Neu Isenburg	09.09.2019	50.0671452	8.7042427	hSouth		
S_205	damaged	Wegscheide	10.09.2019	50.2076	9.4126			x
S_206	healthy	Wegscheide	10.09.2019	50.2076	9.4126			x
S_207	damaged	Wegscheide	10.09.2019	50.2076	9.4126	dSouth		
S_208	healthy	Wegscheide	10.09.2019	50.2076	9.4126	hSouth		
S_209	damaged	Wegscheide	10.09.2019	50.2149354	9.419513	dSouth		
S_210	healthy	Wegscheide	10.09.2019	50.2149354	9.419513	hSouth		
S_211	damaged	Wegscheide	10.09.2019	50.2114485	9.409662	dSouth		
S_212	healthy	Wegscheide	10.09.2019	50.2114485	9.409662	hSouth		
S_213	damaged	Wegscheide	10.09.2019	50.2114485	9.409662	dSouth		
S_214	healthy	Wegscheide	10.09.2019	50.2114485	9.409662	hSouth		
S_215	damaged	Wegscheide	10.09.2019	50.2109	9.4086	dSouth		
S_216	healthy	Wegscheide	10.09.2019	50.2109	9.4086	hSouth		
S_217	damaged	Waldstadion	10.09.2019	50.0546504	8.6626215	dSouth		
S_218	healthy	Waldstadion	10.09.2019	50.0546504	8.6626215	hSouth		
S_219	damaged	Waldstadion	10.09.2019	50.0555269	8.6618698	dSouth		
S_220	healthy	Waldstadion	10.09.2019	50.0555269	8.6618698	hSouth		
S_221	damaged	Waldstadion	10.09.2019	50.0568445	8.6610993	dSouth		
S_222	healthy	Waldstadion	10.09.2019	50.0568445	8.6610993	hSouth		
S_223	damaged	Waldstadion	10.09.2019	50.0572346	8.6619006	dSouth		
S_224	healthy	Waldstadion	10.09.2019	50.0572346	8.6619006	hSouth		
S_225	damaged	Waldstadion	10.09.2019	50.0573499	8.661843	dSouth		

S_226	healthy	Waldstadion	10.09.2019	50.0573499	8.661843	hSouth		
S_227	damaged	Waldstadion	10.09.2019	50.0589663	8.6609092	dSouth		
S_228	healthy	Waldstadion	10.09.2019	50.0589663	8.6609092	hSouth		
S_229	damaged	Waldstadion	10.09.2019	50.0587827	8.6609424	dSouth		
S_230	healthy	Waldstadion	10.09.2019	50.0587827	8.6609424	hSouth		
S_231	damaged	Messel	11.09.2019	49.9648055	8.7305273	dSouth		
S_232	healthy	Messel	11.09.2019	49.9648055	8.7305273	hSouth		
S_233	damaged	Messel	11.09.2019	49.9653231	8.7286833	dSouth		
S_234	healthy	Messel	11.09.2019	49.9653231	8.7286833	hSouth		
S_235	damaged	Messel	11.09.2019	49.9672891	8.7267089	dSouth		
S_236	healthy	Messel	11.09.2019	49.9672891	8.7267089	hSouth		
S_237	damaged	Messel	11.09.2019	49.9673648	8.726613	dSouth		
S_238	healthy	Messel	11.09.2019	49.9673648	8.726613	hSouth		
S_239	damaged	Messel	11.09.2019	49.9685641	8.7259826	dSouth		
S_240	healthy	Messel	11.09.2019	49.9685641	8.7259826	hSouth		
S_241	damaged	Messel	11.09.2019	49.9702459	8.7244602	dSouth		
S_242	healthy	Messel	11.09.2019	49.9702459	8.7244602	hSouth		
S_243	damaged	Messel	11.09.2019	49.9722449	8.7156846	dSouth		
S_244	healthy	Messel	11.09.2019	49.9722449	8.7156846	hSouth		
S_245	damaged	Messel	11.09.2019	49.9722449	8.7156806			x
S_246	healthy	Messel	11.09.2019	49.9722449	8.7156806			x
S_247	damaged	Messel	11.09.2019	49.9724476	8.7142302	dSouth		
S_248	healthy	Messel	11.09.2019	49.9724476	8.7142302	hSouth		
S_249	damaged	Messel	11.09.2019	49.9718971	8.7119104	dSouth		
S_250	healthy	Messel	11.09.2019	49.9718971	8.7119104	hSouth		
S_251	damaged	Messel	11.09.2019	49.9719081	8.7114799	dSouth		
S_252	healthy	Messel	11.09.2019	49.9719081	8.7114799	hSouth		
S_253	damaged	Lorsch	12.09.2019	49.6491886	8.5376088	dSouth		
S_254	healthy	Lorsch	12.09.2019	49.6491886	8.5376088	hSouth		
S_255	damaged	Lorsch	12.09.2019	49.6493532	8.5369721	dSouth		
S_256	healthy	Lorsch	12.09.2019	49.6493532	8.5369721	hSouth		
S_257	damaged	Lorsch	12.09.2019	49.6488428	8.5381241	dSouth		
S_258	healthy	Lorsch	12.09.2019	49.6488428	8.5381241	hSouth		
S_259	damaged	Lorsch	12.09.2019	49.6485083	8.5392349	dSouth		
S_260	healthy	Lorsch	12.09.2019	49.6485083	8.5392349	hSouth		
S_261	damaged	Lorsch	12.09.2019	49.6481419	8.5395785	dSouth		
S_262	healthy	Lorsch	12.09.2019	49.6481419	8.5395785	hSouth		
S_263	damaged	Lorsch	12.09.2019	49.6462656	8.5421035	dSouth		
S_264	healthy	Lorsch	12.09.2019	49.6462656	8.5421035	hSouth		
S_265	damaged	Lorsch	12.09.2019	49.6464364	8.5415305			x
S_266	healthy	Lorsch	12.09.2019	49.6464364	8.5415305			x
S_267	damaged	Lorsch	12.09.2019	49.6463205	8.5410504	dSouth		
S_268	healthy	Lorsch	12.09.2019	49.6463205	8.5410504	hSouth		
S_269	damaged	Lorsch	12.09.2019	49.6452786	8.5358174	dSouth		
S_270	healthy	Lorsch	12.09.2019	49.6452786	8.5358174	hSouth		
S_271	damaged	Lorsch	12.09.2019	49.6451675	8.5351421	dSouth		
S_272	healthy	Lorsch	12.09.2019	49.6451675	8.5351421	hSouth		
S_273	damaged	Lorsch	12.09.2019	49.649297	8.5362281			x
S_274	healthy	Lorsch	12.09.2019	49.649297	8.5362281			x
S_275	damaged	Lorsch	12.09.2019	49.6494678	8.5366794	dSouth		
S_276	healthy	Lorsch	12.09.2019	49.6494678	8.5366794	hSouth		
S_277	damaged	Heusenstamm	13.09.2019	50.0580508	8.7747529	dSouth		
S_278	healthy	Heusenstamm	13.09.2019	50.0580508	8.7747529	hSouth		
S_279	damaged	Heusenstamm	13.09.2019	50.0580635	8.7746208			x
S_280	healthy	Heusenstamm	13.09.2019	50.0580635	8.7746208			x
S_281	damaged	Heusenstamm	13.09.2019	50.057182	8.773846	dSouth		
S_282	healthy	Heusenstamm	13.09.2019	50.057182	8.773846	hSouth		
S_283	damaged	Heusenstamm	13.09.2019	50.0571046	8.7740264	dSouth		
S_284	healthy	Heusenstamm	13.09.2019	50.0571046	8.7740264	hSouth		
S_285	damaged	Heusenstamm	13.09.2019	50.0566422	8.7736616	dSouth		
S_286	healthy	Heusenstamm	13.09.2019	50.0566422	8.7736616	hSouth		
S_287	damaged	Heusenstamm	13.09.2019	50.0561296	8.7732438	dSouth		
S_288	healthy	Heusenstamm	13.09.2019	50.0561296	8.7732438	hSouth		
S_289	damaged	Heusenstamm	13.09.2019	50.0559955	8.7728465	dSouth		
S_290	healthy	Heusenstamm	13.09.2019	50.0559955	8.7728465	hSouth		
S_291	damaged	Heusenstamm	13.09.2019	50.055472	8.7729314	dSouth		
S_292	healthy	Heusenstamm	13.09.2019	50.055472	8.7729314	hSouth		
S_293	damaged	Heusenstamm	13.09.2019	50.055181	8.772228	dSouth		

S_294	healthy	Heusenstamm	13.09.2019	50.055181	8.772228	hSouth		
S_295	damaged	Heusenstamm	13.09.2019	50.0551293	8.7723349	dSouth		
S_296	healthy	Heusenstamm	13.09.2019	50.0551293	8.7723349	hSouth		
S_297	damaged	Heusenstamm	13.09.2019	50.0549188	8.7721502	dSouth		
S_298	healthy	Heusenstamm	13.09.2019	50.0549188	8.7721502	hSouth		
S_299	damaged	Heusenstamm	13.09.2019	50.0548086	8.7726598			x
S_300	healthy	Heusenstamm	13.09.2019	50.0548086	8.7726598			x
conf_001	damaged	Schloßborn	03.08.2020	50.1904623	8.373935			
conf_002	healthy	Schloßborn	03.08.2020	50.1902617	8.3738026			x
conf_003	damaged	Schloßborn	03.08.2020	50.1887401	8.372701			
conf_004	healthy	Schloßborn	03.08.2020	50.1879031	8.3716613			x
conf_005	damaged	Schloßborn	03.08.2020	50.1865722	8.3710684			x
conf_006	healthy	Schloßborn	03.08.2020	50.18656127	8.3711265			x
conf_007	damaged	Schloßborn	03.08.2020	50.1857023	8.3708097			x
conf_008	healthy	Schloßborn	03.08.2020	50.1851555	8.3712359			x
conf_009	damaged	Schloßborn	03.08.2020	50.1852938	8.371852			x
conf_010	healthy	Schloßborn	03.08.2020	50.1851807	8.3722412			x
conf_011	healthy	Schloßborn	03.08.2020	50.1864421	8.3767229			x
conf_012	damaged	Schloßborn	03.08.2020	50.1864287	8.3764222			x
conf_013	damaged	Ruppertshain	04.08.2020	50.181629	8.4018675			x
conf_014	healthy	Ruppertshain	04.08.2020	50.1815555	8.4018799			x
conf_016	healthy	Ruppertshain	04.08.2020	50.1818417	8.4023975			x
conf_017	damaged	Ruppertshain	04.08.2020	50.1846569	8.4022888			x
conf_018	healthy	Ruppertshain	04.08.2020	50.1847183	8.40225810			x
conf_019	damaged	Ruppertshain	04.08.2020	50.1867665	8.4029614			x
conf_020	healthy	Ruppertshain	04.08.2020	50.1868466	8.4029997			x
conf_021	damaged	Ruppertshain	04.08.2020	50.1868411	8.4040772			x
conf_022	healthy	Ruppertshain	04.08.2020	50.1877796	8.4046797			x
conf_023	damaged	Ruppertshain	04.08.2020	50.1829212	8.3987642			x
conf_024	healthy	Ruppertshain	04.08.2020	50.182956	8.3987399			x
conf_025	damaged	Ruppertshain	04.08.2020	50.1808246	8.3990728			x
conf_026	healthy	Ruppertshain	04.08.2020	50.1806971	8.39899759			x
conf_027	damaged	Ruppertshain	04.08.2020	50.179967	8.3994577			x
conf_028	healthy	Ruppertshain	04.08.2020	50.1798082	8.399525			x
conf_029	damaged	Ruppertshain	04.08.2020	50.1782612	8.3999872			x
conf_030	healthy	Ruppertshain	04.08.2020	50.1782916	8.4002846			x
conf_032	healthy	Falkenstein	05.08.2020	50.201454	8.4872785			x
conf_033	damaged	Falkenstein	05.08.2020	50.2015038	8.4874409			x
conf_034	damaged	Falkenstein	05.08.2020	50.201115	8.4876516			x
conf_036	healthy	Falkenstein	05.08.2020	50.2018627	8.4875841			x
conf_037	damaged	Falkenstein	05.08.2020	50.2011419	8.4892266			x
conf_038	healthy	Falkenstein	05.08.2020	50.2012289	8.489425			x
conf_039	healthy	Falkenstein	05.08.2020	50.2013307	8.4905266			
conf_040	damaged	Falkenstein	05.08.2020	50.2004517	8.4905881			x
conf_041	healthy	Falkenstein	05.08.2020	50.2008376	8.4909408			x
conf_042	damaged	Falkenstein	05.08.2020	50.20009229	8.4909295			x
conf_043	damaged	Falkenstein	05.08.2020	50.1997086	8.4828883			x
conf_045	healthy	Falkenstein	05.08.2020	50.1992717	8.480502			x
conf_046	damaged	Falkenstein	05.08.2020	50.1995271	8.4806157			x
conf_047	healthy	Falkenstein	05.08.2020	50.1995032	8.4806215			x
conf_050	damaged	Rote Mühle	07.08.2020	50.1612598	8.452304			x
conf_051	healthy	Rote Mühle	07.08.2020	50.1610649	8.4526065			x
conf_052	damaged	Rote Mühle	07.08.2020	50.1611651	8.4520887			x
conf_053	healthy	Rote Mühle	07.08.2020	50.1611113	8.4520672			x
conf_054	damaged	Rote Mühle	07.08.2020	50.1611776	8.4511498			x
conf_055	healthy	Rote Mühle	07.08.2020	50.1611331	8.450964			x
conf_056	damaged	Rote Mühle	07.08.2020	50.1612598	8.4508452			x
conf_057	healthy	Rote Mühle	07.08.2020	50.1614085	8.4509926			x
conf_058	damaged	Rote Mühle	07.08.2020	50.1617899	8.4504762			x
conf_059	healthy	Rote Mühle	07.08.2020	50.1617076	8.4505298			x

Suppl. Table 2.Results from Mann-Whitney U-test on difference between damaged and healthy trees sampled.

Parameter	Mann-Whitney U	p
trunk circumference	10718	0.48
tree height	9874	0.27
canopy closure	10820	0.56
competition index	10809	0.57
dried leaves	202	<0.001
leaf loss	352	<0.001

Suppl. Fig.1. Climate change dynamics. Mean change of sampling site values along PCA axis 1 (temperature, red) and PCA axis 2 (precipitation, blue) among decades.

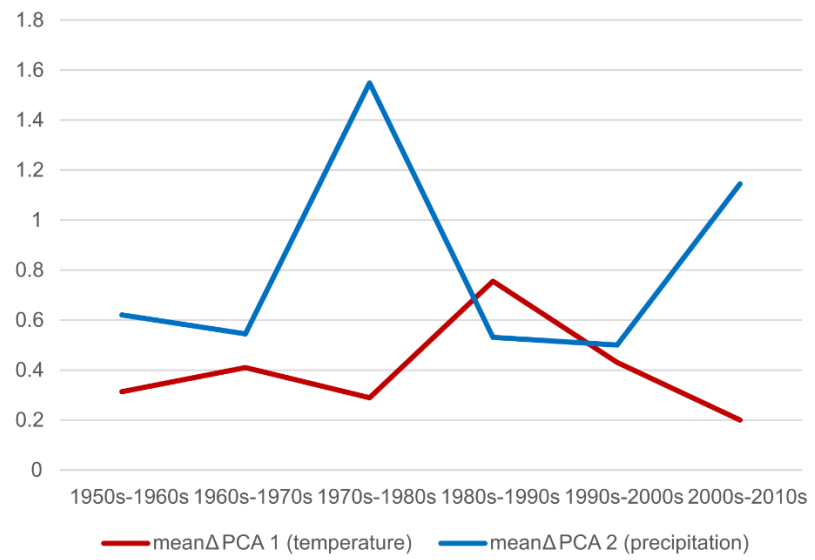

Suppl. Fig. 2. Genomic similarity among individuals within and among phenotypic classes. Permutation ANOSIM shows that the differences are not significant (p = 0.76).

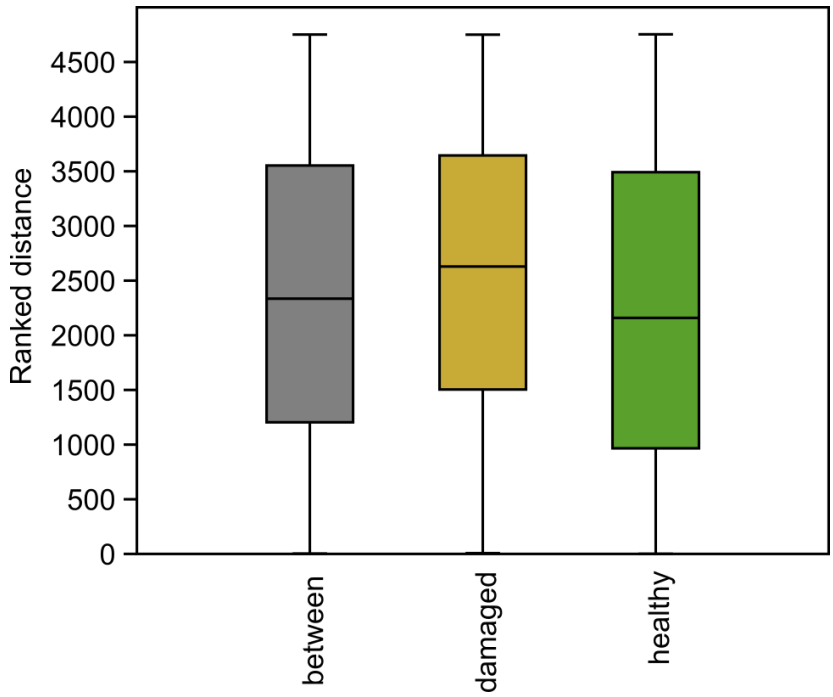

Suppl. Fig. 3. A) Manhattan plot of uncorrected p values from CMH test and B) corresponding QQ-plot. SNPs on different chromosomes are alternatingly coloured blue and black.

A)

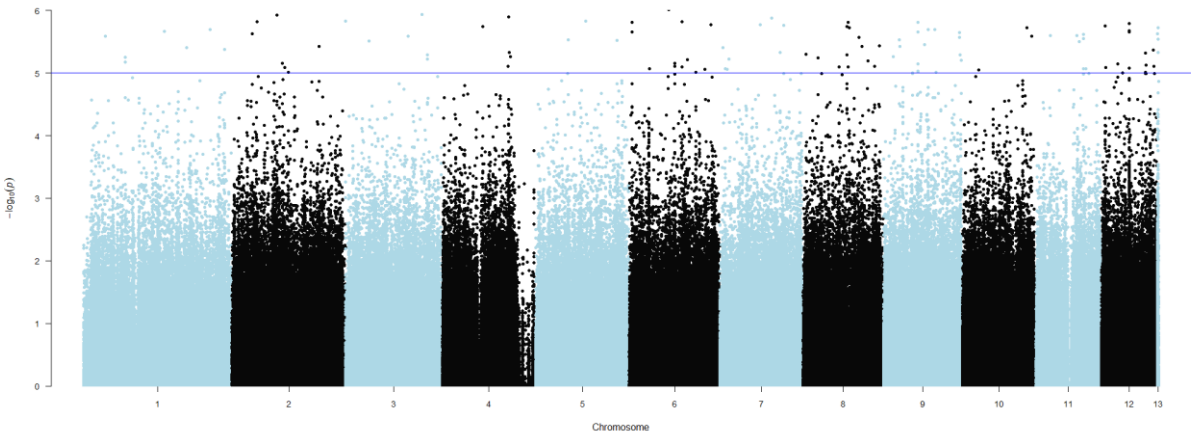

B)

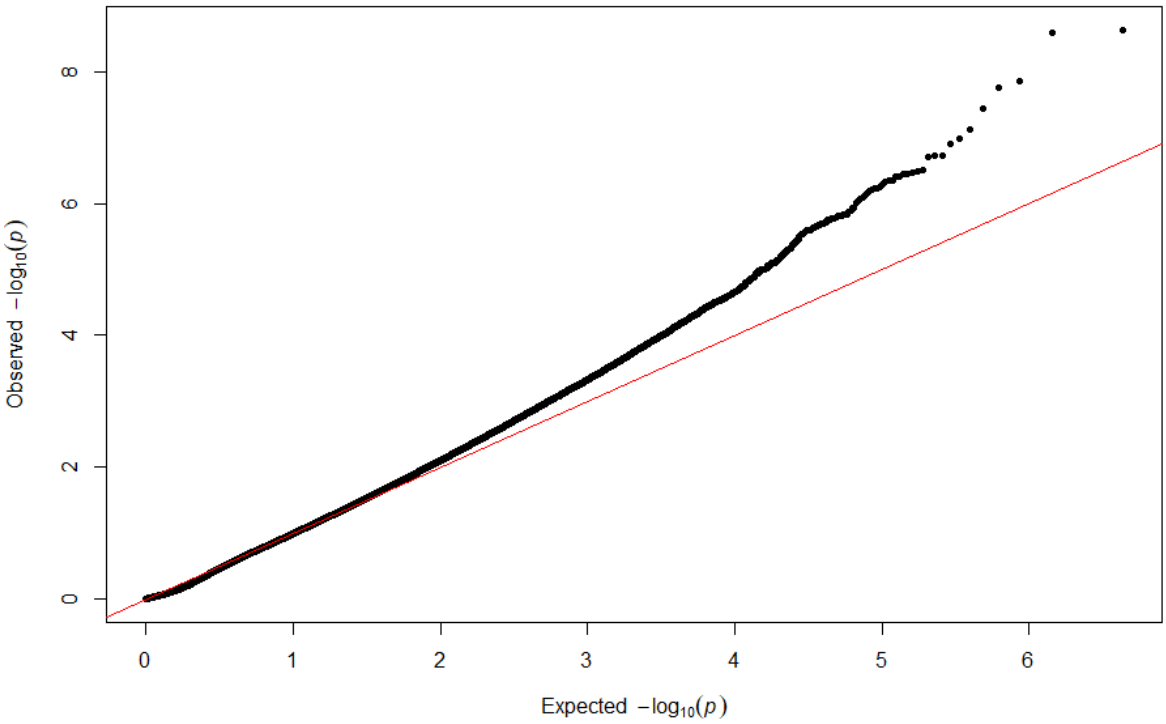

Suppl. Fig. 4. Increase of prediction success with the number of loci involved. Loci were added according to their decreasing contribution in the final analysis.

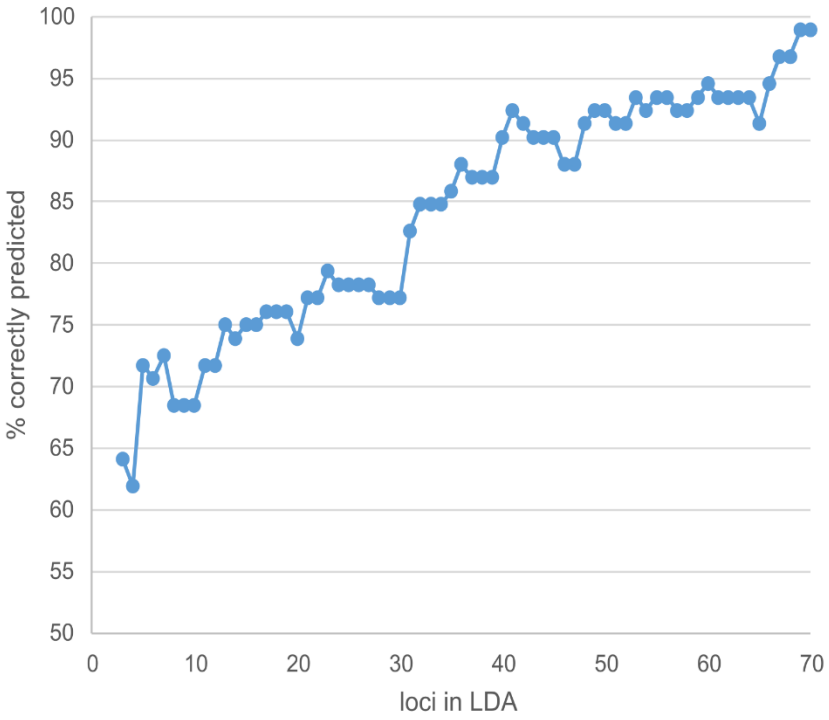

Suppl. Fig. 5. Comparison of observed heterozygosity between lower and upper half of predictive values “healthy” in DA. The medians are not significantly different (Mann-Whitney U = 293.5, p same median = 0.72).

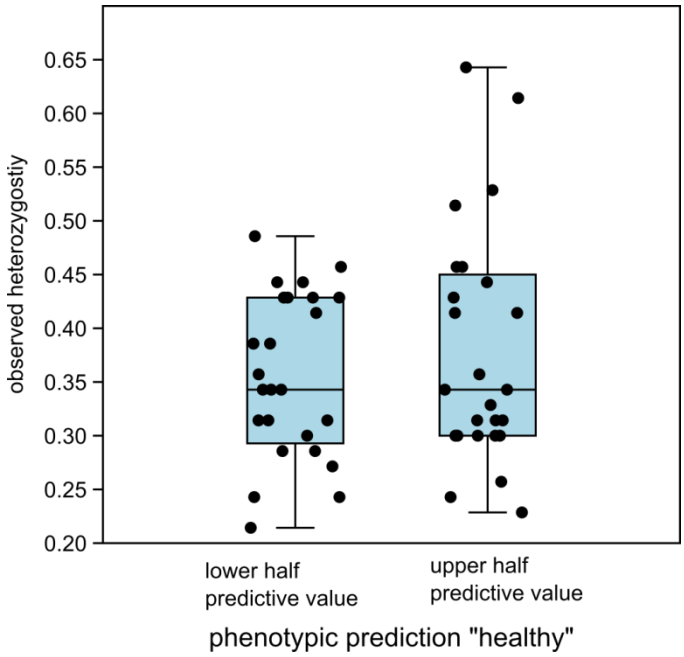

Suppl. Fig.6. Histogram of LDA results. Individuals, where the predicted phenotype did not match the observed phenotype are shown in grey, individuals with matching observed/predicted phenotype in green (healthy) or in ochre (damaged).

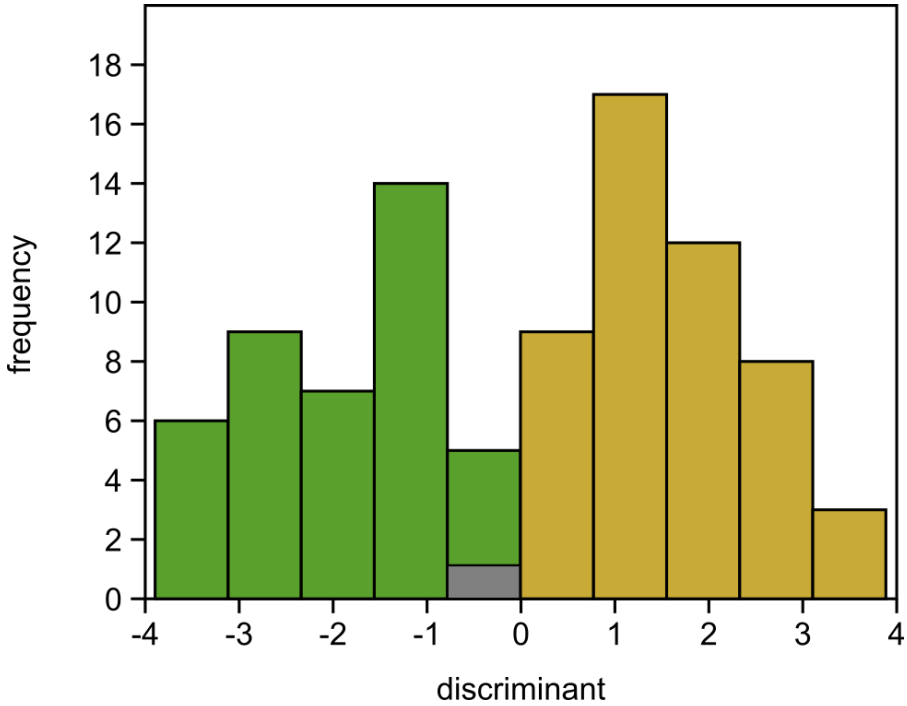

Suppl. Table 2. List of genes with significant SNPs. Functional annotations and relation to drought phenotype are given whenever available.

***F. sylvatica* gene ID**	**Best BLAST hit ID**	**BLAST hit protein name**	**taxon**	**UniProt ID**	**UniProt protein name**	**function (UniProt)**	**citation function**	**relation to drought phenotype**	**citation**
1.g3851.t1	KUM50718.1	hypothetical protein ABT39_MTgene562	*Picea glauca*	none	-	-	-	-	-
10.g3914.t1	XP_023883481.1	uncharacterized protein LOC111995782 isoform X1	*Quercus suber*	none	-	-	-	-	-
11.g2467.t1	XP_023923514.1	exosome complex exonuclease RRP46 homolog isoform X1	*Quercus suber*	EXOS5_ORYSJ	Exosome complex exonuclease RRP46 homolog	mRNA degradation	Xiang, D., Yang, H., Venglat, P., Cao, Y., Wen, R., Ren, M., ... & Weijers, D. (2011). POPCORN functions in the auxin pathway to regulate embryonic body plan and meristem organization in Arabidopsis. The Plant Cell, 23(12), 4348-4367.	-	-
11.g2832.t1	XP_030949821.1	WD repeat-containing protein PCN-like	*Quercus lobata*	PCN_ARATH	WD repeat-containing protein PCN	Involved in auxin signalling pathway. Required for embryo development and meristem	-	drought stress response	Park, S. R., Hwang, J., & Kim, M. (2020). The Arabidopsis WDR55 is positively involved in ABA-mediated drought tolerance response.

						organization. Functions in the auxin pathway, integrating auxin signalling in the organization and maintenance of the shoot apical meristem (SAM) and root apical meristem (RAM).			Plant Biotechnology Reports, 1-12.
12.g1695.t1	XP_030973623.1	uncharacterized protein LOC115993791	*Quercus lobata*	F4I5S1_ARATH	PB1 domain-containing protein tyrosine kinase	not well characterised	-	-	-
2.g4736.t1	KAF3975221.1	hypothetical protein CMV_001513	*Castanea mollissima*	none	-	-	-	-	-
3.g3590.t1	XP_030942104.1	uncharacterized protein LOC115967180	*Quercus lobata*	none	-	-	-	-	-
4.g3980.t1	XP_030950630.1	cytokinin dehydrogenase 5	*Quercus lobata*	CKX1_ARATH	Cytokinin dehydrogenase 1	Catalyzes the oxidation of cytokinins, a family of N6-substituted adenine derivatives that are plant hormones, where the substituent is an isopentenyl group.	Werner, T., Motyka, V., Laucou, V., Smets, R., Van Onckelen, H., & Schmülling, T. (2003). Cytokinin-deficient transgenic Arabidopsis plants show multiple developmental alterations indicating opposite functions of cytokinins in the regulation	drought stress response	Emery, R. J., & Kisiala, A. (2020). The Roles of Cytokinins in Plants and Their Response to Environmental Stimuli. Li, W., Herrera-Estrella, L., & Tran, L. S. P. (2016). The Yin–Yang of cytokinin homeostasis and drought acclimation/adaptation. Trends in Plant Science, 21(7), 548-550.

							of shoot and root meristem activity. The Plant Cell, 15(11), 2532-2550.		
5.g1807.t1	XP_030939294.1	guanosine nucleotide diphosphate dissociation inhibitor 2	*Quercus lobata*	GDI2_ARATH	Guanosine nucleotide diphosphate dissociation inhibitor 2	Regulates the GDP/GTP exchange reaction of most RAB proteins by inhibiting the dissociation of GDP from them, and the subsequent binding of GTP.	Ueda, T., Yoshizumi, T., Anai, T., Matsui, M., Uchimiya, H., & Nakano, A. (1998). AtGDI2, a novel Arabidopsis gene encoding a Rab GDP dissociation inhibitor. Gene, 206(1), 137-143.	environmental stress response	Carvalho, B. M., Viana, A. P., dos Santos, P. H. D., Generoso, A. L., Corrêa, C. C. G., Silveira, V., ... & Santos, E. A. (2019). Proteome of resistant and susceptible Passiflora species in the interaction with cowpea aphid-borne mosaic virus reveals distinct responses to pathogenesis. Euphytica, 215(10), 167.
6.g2227.t1	THG21676.1	hypothetical protein TEA_000305	*Camellia sinensis* var. *sinensis*	NDUS7_ARATH	NADH dehydrogenase [ubiquinone] iron-sulfur protein 7, mitochondrial	Core subunit of the mitochondrial membrane respiratory chain NADH dehydrogenase (Complex I) that is believed to belong to the minimal assembly required for catalysis. Complex I functions in the transfer of electrons from NADH to the		drought stress response	Zhang, S., Zhang, L., Zhou, K., Li, Y., & Zhao, Z. (2017). Changes in protein profile of Platycladus orientalis (L.) roots and leaves in response to drought stress. Tree Genetics & Genomes, 13(4), 76.

						respiratory chain. The immediate electron acceptor for the enzyme is believed to be ubiquinone			
6.g2921.t1	KAB1222126.1	Ribonuclease H2 subunit C	*Morella rubra*	RNH2A_ARATH	Ribonuclease H2 subunit A	Catalytic subunit of RNase HII, an endonuclease that specifically degrades the RNA of RNA:DNA hybrids. Participates in DNA replication, possibly by mediating the removal of lagging-strand Okazaki fragment RNA primers during DNA replication. Mediates the excision of single ribonucleotides from DNA:RNA duplexes	-	-	-
7.g177.t1	XP_018842121.1	PREDICTED: tubby-like F-box protein 8 isoform X1	*Juglans regia*	TLP10_ARATH	Tubby-like F-box protein 10	Component of SCF(ASK-cullin-F-box) E3 ubiquitin ligase complexes, which may mediate the ubiquitination and subsequent proteasomal	-	drought stress response	Xu, J., Xing, S., Sun, Q., Zhan, C., Liu, X., Zhang, S., & Wang, X. (2019). The expression of a tubby-like protein from Malus domestica (Md TLP7) enhances abiotic stress tolerance in Arabidopsis. BMC plant biology, 19(1), 1-8.

						degradation of target proteins			
7.g2350.t1	KAF3966828.1	hypothetical protein CMV_009102	*Castanea mollissima*	PRK4_ARATH	Pollen receptor-like kinase 4	Receptor-like kinase involved in the control of pollen germination and pollen tube polar growth. Can phosphorylate ROPGEF1 in vitro	Chang, F., Gu, Y., Ma, H., & Yang, Z. (2013). AtPRK2 promotes ROP1 activation via RopGEFs in the control of polarized pollen tube growth. Molecular plant, 6(4), 1187-1201.	environmental stress response	Guo, J., Dong, X., Li, Y., & Wang, B. (2020). NaCl treatment markedly enhanced pollen viability and pollen preservation time of euhalophyte Suaeda salsa via up regulation of pollen development-related genes. Journal of plant research, 133(1), 57-71.
7.g3617.t1	XP_023924613.1	protein LIGHT-DEPENDENT SHORT HYPOCOTYLS 10-like isoform X1	*Quercus suber*	LSH4_ARATH	Protein LIGHT-DEPENDENT SHORT HYPOCOTYLS 4	Probable transcription regulator that acts as a developmental regulator by promoting cell growth in response to light. May suppress organ differentiation in the boundary region	Takeda, S., Hanano, K., Kariya, A., Shimizu, S., Zhao, L., Matsui, M., ... & Aida, M. (2011). CUP-SHAPED COTYLEDON1 transcription factor activates the expression of LSH4 and LSH3, two members of the ALOG gene family, in shoot organ boundary cells. The Plant Journal, 66(6), 1066-1077.	-	

7.g3816.t1	XP_018811587.1	ethylene-responsive transcription factor 12-like	*Juglans regia*	TAFCL_ARATH	Transcription initiation factor TFIID subunit 12b	TAFs are components of the transcription factor IID (TFIID) complex that is essential for mediating regulation of RNA polymerase transcription. Required for the expression of a subset of ethylene-responsive genes (By similarity). Involved in the negative regulation of cytokinin sensitivity	-	-	-
7.g552.t1	No hits found		-	-	-	-	-	-	-
8.g3494.t1	XP_022750437.1	V-type proton ATPase subunit C	*Durio zibethinus*	VATC_ARATH	V-type proton ATPase subunit C	Subunit of the peripheral V1 complex of vacuolar ATPase. Subunit C is necessary for the assembly of the catalytic sector of the enzyme and is likely to have a specific function in its catalytic activity. V-ATPase is responsible for acidifying a variety of intracellular	-	drought stress response	Kausar, R., Arshad, M., Shahzad, A., & Komatsu, S. (2013). Proteomics analysis of sensitive and tolerant barley genotypes under drought stress. Amino Acids, 44(2), 345-359. Li, J., Jia, H., Han, X., Zhang, J., Sun, P., Lu, M., & Hu, J. (2016). Selection of reliable reference genes for gene expression analysis under abiotic stresses in the desert biomass willow, *Salix psammophila*. Frontiers

						compartments in eukaryotic cells			in plant science, 7, 1505.
9.g3080.t1	XP_030929046.1	probable inactive purple acid phosphatase 29	*Quercus lobata*	PPA14_ARATH	Probable inactive purple acid phosphatase 14	-	-	drought stress response	Street, N. R., Skogström, O., Sjödin, A., Tucker, J., Rodríguez-Acosta, M., Nilsson, P., ... & Taylor, G. (2006). The genetics and genomics of the drought response in Populus. The Plant Journal, 48(3), 321-341. Prinsi, B., Negri, A. S., Failla, O., Scienza, A., & Espen, L. (2018). Root proteomic and metabolic analyses reveal specific responses to drought stress in differently tolerant grapevine rootstocks. BMC plant biology, 18(1), 126.
9.g4504.t1	KAF3976808.1	hypothetical protein CMV_000062	*Castanea mollissima*	TBL33_ARATH	Protein trichome birefringence-like 33	Probable xylan acetyltransferase that plays a role in xylan acetylation and normal deposition of secondary cell walls	Yuan, Y., Teng, Q., Zhong, R., Haghighat, M., Richardson, E. A., & Ye, Z. H. (2016). Mutations of Arabidopsis TBL32 and TBL33 affect xylan acetylation and secondary wall deposition. PLoS One, 11(1), e0146460.	drought stress response	Shuai, P., Liang, D., Zhang, Z., Yin, W., & Xia, X. (2013). Identification of drought-responsive and novel Populus trichocarpamicroRNAs by high-throughput sequencing and their targets using degradome analysis. Bmc Genomics, 14(1), 233.

Suppl. Table . List of genes closest to significant SNPs. Functional annotations and relation to drought phenotype are given whenever available.

***F. sylvatica* gene ID**	**Best BLAST hit ID**	**BLAST hit protein name**	**taxon**	**UniProt ID**	**UniProt protein name**	**function (UniProt)**	**citation function**	**relation to drought phenotype**	**citation**
Backbone_621.g33	KAF3957547	hypothetical protein CMV_017449	*Castanea mollissima*						
Backbone_621.g49	XP_030932040	pathogen-related protein	*Quercus lobata*						
1.g1111	KAF3976566	hypothetical protein CMV_000247	*Castanea mollissima*	ACBP4_ARATH	Acyl-CoA-binding domain-containing protein 4	Binds medium- and long-chain acyl-CoA esters with very high affinity. Can interact in vitro with oleoyl-CoA, barely with palmitoyl-CoA, but not with arachidonyl-CoA.	Leung, K. C., Li, H. Y., Mishra, G., & Chye, M. L. (2005). ACBP4 and ACBP5, novel Arabidopsis acyl-CoA-binding proteins with kelch motifs that bind oleoyl-CoA. Plant molecular biology, 55(2), 297-309.	environmental stress response	Du, Z. Y., Arias, T., Meng, W., & Chye, M. L. (2016). Plant acyl-CoA-binding proteins: an emerging family involved in plant development and stress responses. Progress in Lipid Research, 63, 165-181.
1.g2051	XP_031256586	aspartic proteinase nepenthesin-1-like	*Pistacia vera*					drought stress response	Prinsi, B., Negri, A. S., Failla, O., Scienza, A., & Espen, L. (2018). Root proteomic and metabolic analyses reveal specific responses to drought stress in differently tolerant grapevine rootstocks. BMC plant biology, 18(1), 126.

1.g5025	No hits found								
1.g6250	XP_030925267	BTB/POZ domain and ankyrin repeat-containing protein NOOT2	*Quercus lobata*	NPR5_ARATH	Regulatory protein NPR5	May act as a substrate-specific adapter of an E3 ubiquitin-protein ligase complex (CUL3-RBX1-BTB) which mediates the ubiquitination and subsequent proteasomal degradation of target proteins	Hepworth, S. R., Zhang, Y., McKim, S., Li, X., & Haughn, G. W. (2005). BLADE-ON-PETIOLE–dependent signaling controls leaf and floral patterning in Arabidopsis. The Plant Cell, 17(5), 1434-1448.		
1.g7050	PQQ17864	insulin-degrading enzyme-like 1 peroxisomal	*Prunus yedoensis*	IDE1_ARATH	insulin-degrading enzyme-like 1 peroxisomal	Peptidase that might be involved in pathogen or wound response.	Lingard, M. J., & Bartel, B. (2009). Arabidopsis LON2 is necessary for peroxisomal function and sustained matrix protein import. Plant physiology, 151(3), 1354-1365.		
2.g1138	XP_018818502	PREDICTED: uncharacterized protein LOC108989373 isoform X3	*Juglans regia*						
2.g1372	KAF3967401	hypothetical protein CMV_008608	*Castanea mollissima*						
2.g1982	No hits found								

2.g4924	TKY55186	Spermine synthase	*Spatholobus suberectus*	SPSY_ARATH	Spermine synthase			drought stress response	Yamaguchi, K., Takahashi, Y., Berberich, T., Imai, A., Takahashi, T., Michael, A. J., & Kusano, T. (2007). A protective role for the polyamine spermine against drought stress in Arabidopsis. Biochemical and biophysical research communications, 352(2), 486-490.
3.g1427	XP_030940223	uncharacterized protein LOC115965177	*Quercus lobata*						
3.g4686	KAF3964003	hypothetical protein CMV_011671	*Castanea mollissima*						
4.g1310	KAF3954505	hypothetical protein CMV_020159	*Castanea mollissima*	Q9C6S8_ARATH	Pre-mRNA-splicing factor of RES complex protein			drought stress response	Qi, Y., Yao, X., Zhao, D., & Lu, L. (2018). Overexpression of SbSKIP, a pre-mRNA splicing factor from Sorghum bicolor, enhances root growth and drought tolerance in Petunia hybrida. Scientia Horticulturae, 240, 281-287.
4.g3868	KAF3971069	hypothetical protein CMV_005309	*Castanea mollissima*						
4.g3915	KAF3976838	hypothetical protein CMV_000012	*Castanea mollissima*						

5.g2789	XP_023898567	uncharacterized protein LOC112010459 isoform X2	*Quercus suber*	Q9M089_ARATH	Keratin-associated protein (DUF1218)			drought stress response	Xu, J., Yuan, Y., Xu, Y., Zhang, G., Guo, X., Wu, F., ... & Tang, Q. (2014). Identification of candidate genes for drought tolerance by whole-genome resequencing in maize. BMC Plant Biology, 14(1), 83.
5.g3716	XP_023870312	dynamin-related protein 5A	*Quercus suber*	DRP5A_ARATH	Dynamin-related protein 5A	Probable microtubule-associated force-producing protein that is targeted to the forming cell plate during cytokinesis. May play a role in cell division	Miyagishima, S. Y., Kuwayama, H., Urushihara, H., & Nakanishi, H. (2008). Evolutionary linkage between eukaryotic cytokinesis and chloroplast division by dynamin proteins. Proceedings of the National Academy of Sciences, 105(39), 15202-15207.	drought stress response	Ren, Z., Zhang, D., Cao, L., Zhang, W., Zheng, H., Liu, Z., ... & Su, H. (2020). Functions and regulatory framework of ZmNST3 in maize under lodging and drought stress. Plant, Cell & Environment, 43(9), 2272-2286.
5.g4697	XP_023901205	cytochrome b561 and DOMON domain-containing protein At4g12980-like	*Quercus suber*						

6.g180	KNA23105	hypothetical protein SOVF_026910	*Spinacia oleracea*						
6.g3229	XP_015867595	transcription initiation factor TFIID subunit 11	*Ziziphus jujuba*	TA14B_ARATH	Transcription initiation factor TFIID	Negative regulator of flowering controlling the H4K5 acetylation levels in the FLC and FT chromatin. Positively regulates FLC expression.	Zacharaki, V., Benhamed, M., Poulios, S., Latrasse, D., Papoutsoglou, P., Delarue, M., & Vlachonasios, K. E. (2012). The Arabidopsis ortholog of the YEATS domain containing protein YAF9a regulates flowering by controlling H4 acetylation levels at the FLC locus. Plant science, 196, 44-52.	drought stress response	Parvathi, M. S., Nataraja, K. N., Reddy, Y. N., Naika, M. B., & Gowda, M. C. (2019). Transcriptome analysis of finger millet (Eleusine coracana (L.) Gaertn.) reveals unique drought responsive genes. Journal of genetics, 98(2), 46.
6.g823	No hits found								
7.g1655	XP_023909357	histone deacetylase 6	*Quercus suber*	HDA6_ARATH	Histone deacetylase 6	Responsible for the deacetylation of lysine residues on the N-terminal part of the core histones (H2A, H2B, H3 and H4).		drought stress response	Kim, J. M., Sasaki, T., Ueda, M., Sako, K., & Seki, M. (2015). Chromatin changes in response to drought, salinity, heat, and cold stresses in plants. Frontiers in plant science, 6, 114.

7.g2958	KAF3966011	hypothetical protein CMV_009858	*Castanea mollissima*	F4I6B2_ARATH	SIT4 phosphatase-associated family protein				
7.g3483	XP_023874962	uncharacterized protein LOC111987473	*Quercus suber*						
7.g3669	XP_023883887	protein trichome birefringence-like 38	*Quercus suber*	TBL38_ARATH	protein trichome birefringence-like 38	May act as a bridging protein that binds pectin and other cell wall polysaccharides. Probably involved in maintaining esterification of pectins		drought stress response	Shuai, P., Liang, D., Zhang, Z., Yin, W., & Xia, X. (2013). Identification of drought-responsive and novel Populus trichocarpamicroRNAs by high-throughput sequencing and their targets using degradome analysis. Bmc Genomics, 14(1), 233.
8.g199	KAF3962723	hypothetical protein CMV_012798	*Castanea mollissima*						
8.g2624	No hits found								
8.g2764	RUS78569	hypothetical protein EGW08_013676, partial	*Elysia chlorotica*						
8.g2926	RUS32681	hypothetical protein BC938DRAFT_474617	*Jimgerdemannia flammicorona*						
8.g3326	XP_030953364	sister chromatid cohesion protein SCC2	*Quercus lobata*	SCC2_ARATH	sister chromatid cohesion protein SCC2	Essential protein required for cell fate determination during embryogenesis	Sebastian, J., Ravi, M., Andreuzza, S., Panoli, A. P., Marimuthu, M. P., & Siddiqi, I.		

							(2009). The plant adherin AtSCC2 is required for embryogenesis and sister-chromatid cohesion during meiosis in Arabidopsis. The Plant Journal, 59(1), 1-13.		
8.g3872	XP_030953755	surfeit locus protein 2	*Quercus lobata*	SURF1_ARATH	Surfeit locus protein 1	Probably involved in the biogenesis of the COX complex			
8.g4454	KAF3955069	hypothetical protein CMV_019673	*Castanea mollissima*						
8.g4554	KAF3975054	hypothetical protein CMV_001659	*Castanea mollissima*						
8.g935	KAF3972759	hypothetical protein CMV_003766	*Castanea mollissima*						
9.g1013	KAF3963767	hypothetical protein CMV_011877	*Castanea mollissima*						
9.g1025	XP_023873320	cytosolic sulfotransferase 5-like	*Quercus suber*						
9.g2127	No hits found								
9.g4398	KAB5561320	hypothetical protein DKX38_006277	*Salix brachista*						

9.g4504	KAF3976808	hypothetical protein CMV_000062	*Castanea mollissima*	TBL33_ARATH	Protein trichome birefringence -like 33	Probable xylan acetyltransferase that plays a role in xylan acetylation and normal deposition of secondary cell walls	Yuan, Y., Teng, Q., Zhong, R., Haghighat, M., Richardson, E. A., & Ye, Z. H. (2016). Mutations of Arabidopsis TBL32 and TBL33 affect xylan acetylation and secondary wall deposition. PLoS One, 11(1), e0146460.	drought stress response	Shuai, P., Liang, D., Zhang, Z., Yin, W., & Xia, X. (2013). Identification of drought-responsive and novel Populus trichocarpamicroRNAs by high-throughput sequencing and their targets using degradome analysis. Bmc Genomics, 14(1), 233.
9.g4548	XP_023928861	uncharacterized protein LOC112040195	*Quercus suber*						
9.g4606	XP_030928366	LOW QUALITY PROTEIN: E3 ubiquitin-protein ligase SHPRH	*Quercus lobata*						
9.g653	KAF3952878	hypothetical protein CMV_021616	*Castanea mollissima*						
10.g4171	ONI05229	hypothetical protein PRUPE_6G363600	*Prunus persica*						
11.g2603	XP_023892377	amino acid permease 6-like	*Quercus suber*	AAP6_ARATH	Amino acid permease 6	Amino acid-proton symporter. Stereospecific transporter with a broad	Rentsch, D., Hirner, B., Schmelzer, E., & Frommer, W. B. (1996). Salt stress-	environmental stress response	Rentsch, D., Hirner, B., Schmelzer, E., & Frommer, W. B. (1996). Salt stress-induced proline transporters and salt

						specificity for tryptophan, proline, and neutral and acidic amino acids.	induced proline transporters and salt stress-repressed broad specificity amino acid permeases identified by suppression of a yeast amino acid permease-targeting mutant. The Plant Cell, 8(8), 1437-1446.		stress-repressed broad specificity amino acid permeases identified by suppression of a yeast amino acid permease-targeting mutant. The Plant Cell, 8(8), 1437-1446.
11.g787	No hits found								
12.g1692	KAF3972258	hypothetical protein CMV_004214	*Castanea mollissima*						
12.g2592	No hits found								
12.g3049	XP_023886583	transcription factor TCP15	*Quercus suber*	TCP15_ARATH	transcription factor TCP15	Transcription factor involved the regulation of plant development. Together with TCP14, modulates plant stature by promoting cell division in young internodes.	Kieffer, M., Master, V., Waites, R., & Davies, B. (2011). TCP14 and TCP15 affect internode length and leaf shape in Arabidopsis. The Plant Journal, 68(1), 147-158.	environmental stress response	Viola, I. L., Camoirano, A., & Gonzalez, D. H. (2016). Redox-dependent modulation of anthocyanin biosynthesis by the TCP transcription factor TCP15 during exposure to high light intensity conditions in Arabidopsis. Plant Physiology, 170(1), 74-85.

12.g922	KAF3957893	hypothetical protein CMV_017140	*Castanea mollissima*						